



TRILATERAL
EUREGIO CLUSTER



JÜLICH
FORSCHUNGSZENTRUM



Diagnostics and control of fusion plasmas

W. Biel^{1,2}

¹Institute of Energy- and Climate Research, Forschungszentrum Jülich GmbH, Germany

²Department of Applied Physics, Ghent University, Belgium

DPG School “The Physics of ITER”

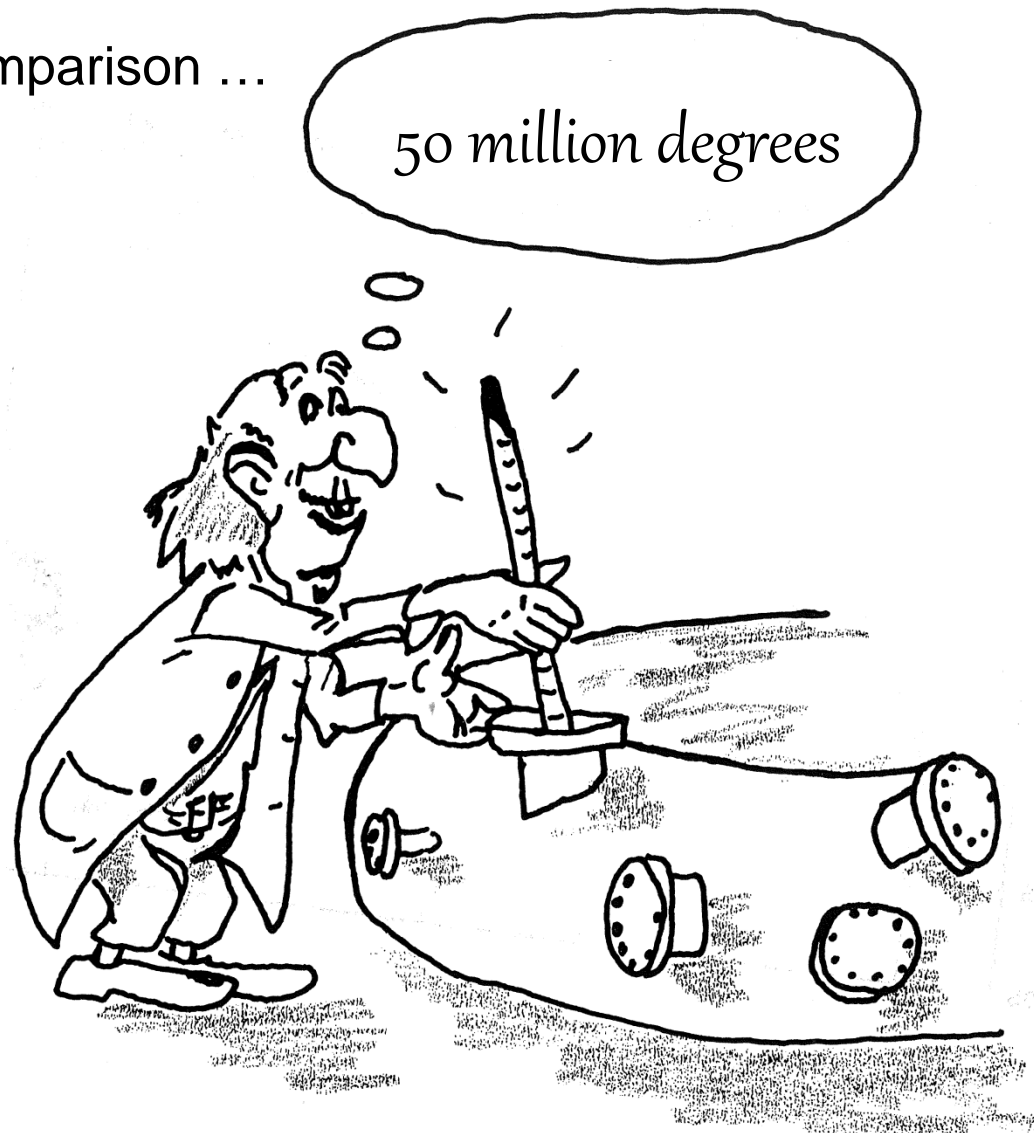
Bad Honnef, 26.09.2014

Measurement means comparison ...



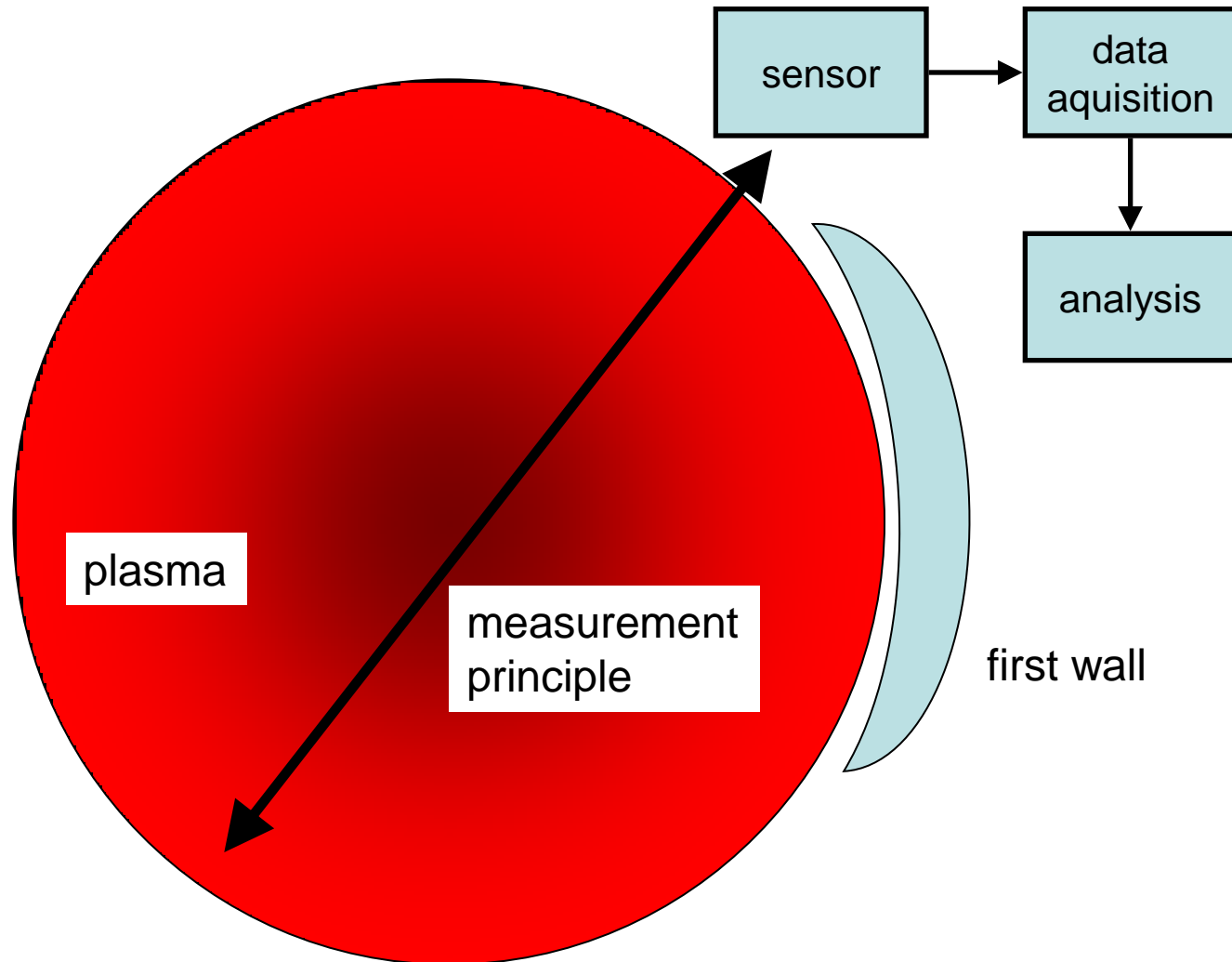
... but how to perform measurements in a hot fusion plasma?

Measurement means comparison ...



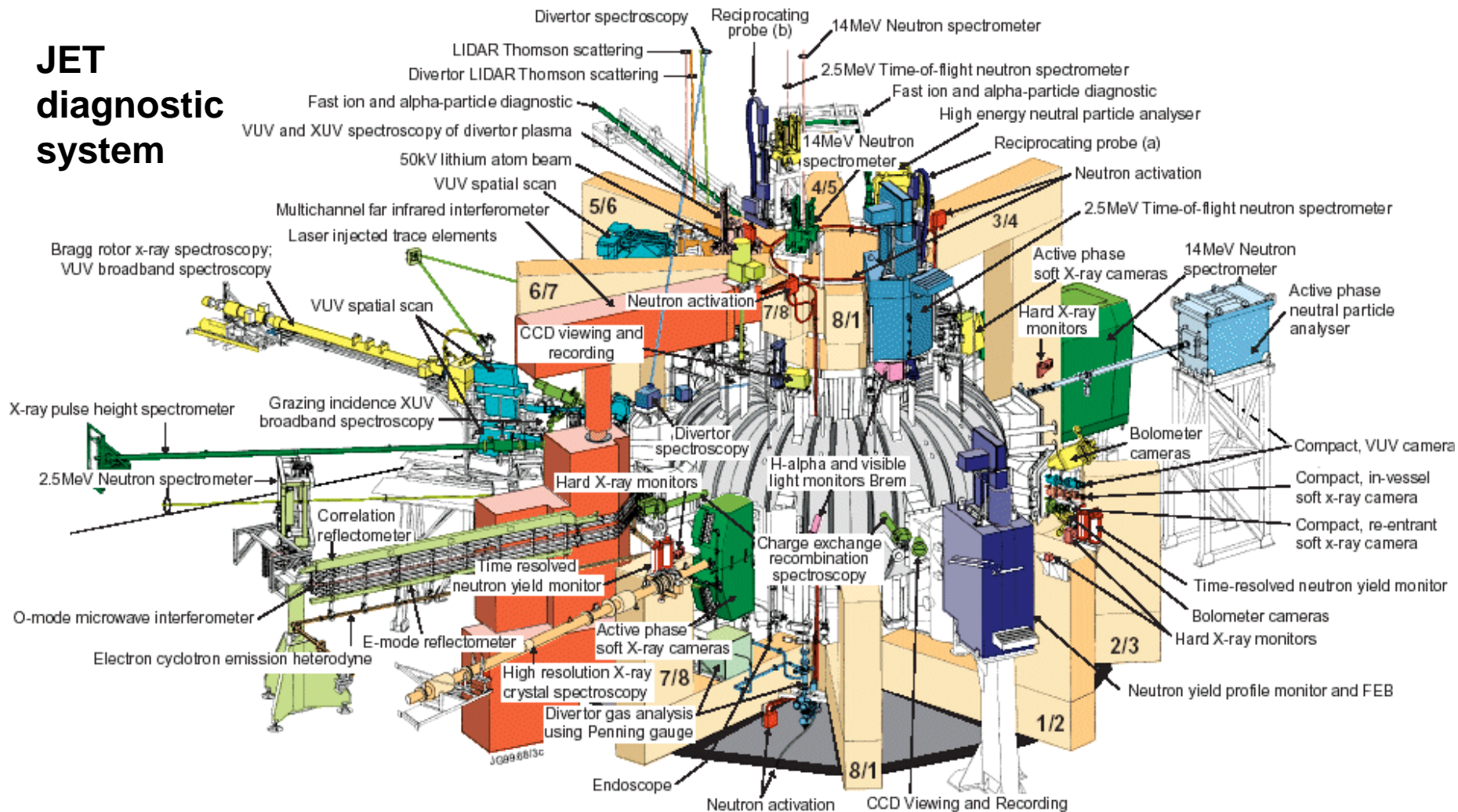
Measurements in a fusion plasma

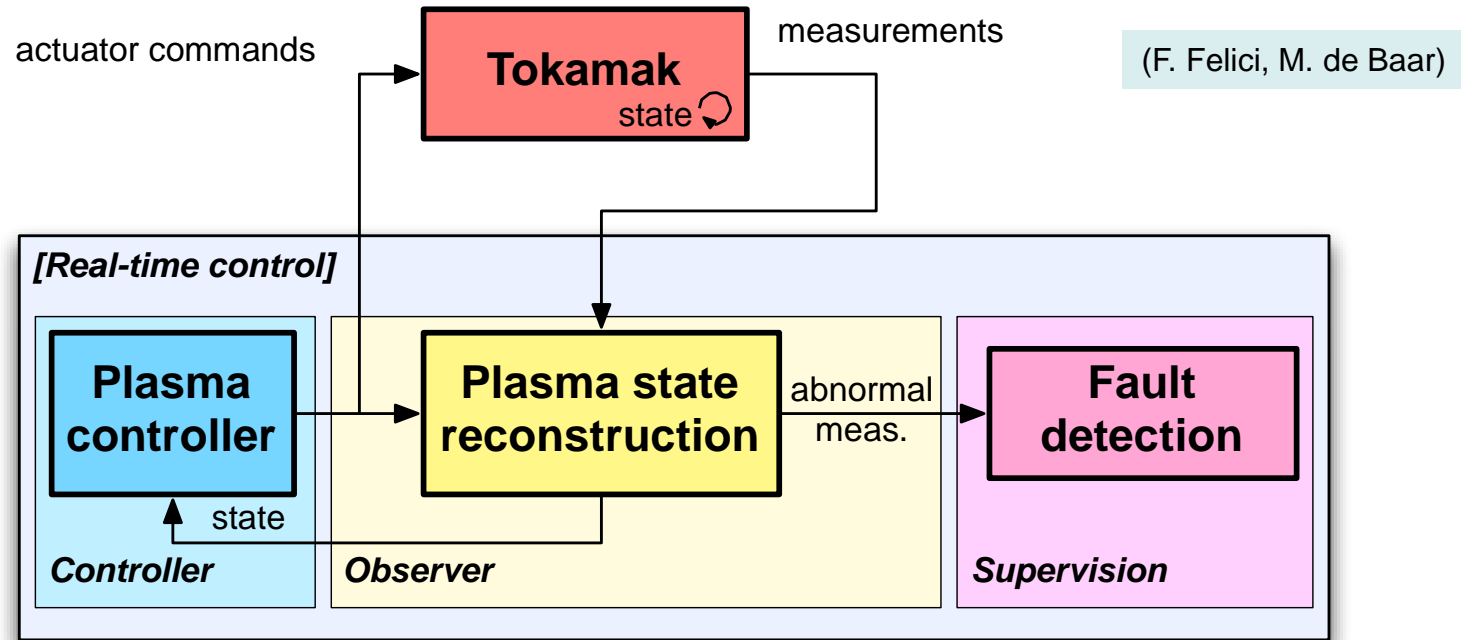
... are generally performed in an indirect way ...



Today's fusion experiments are amply equipped with diagnostic systems ...

JET diagnostic system



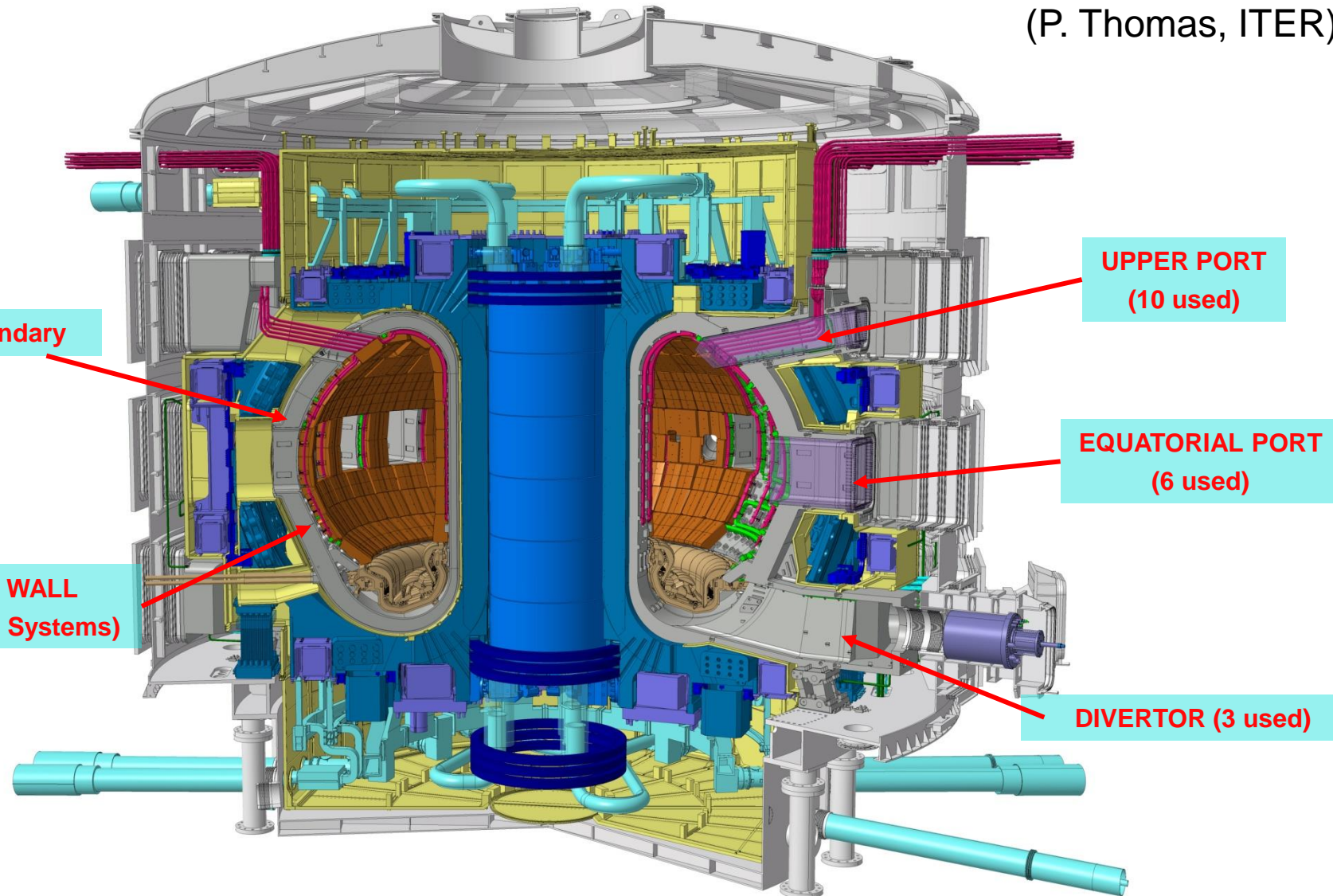


- Plasma controller: perform control actions based on full plasma state knowledge
- Plasma state reconstruction: derive plasma state by merging measurements from several diagnostics
- Fault detection: classify unexpected measurements (e.g. off-normal events, faulty signals)
- Diagnostic redundancy in number of channels and number of methods facilitates handling of faults (the better the model, the less measurements are needed)

- **A) Technical goals of plasma diagnostics:**
 - *Protection of the fusion reactor and its components*
 - e.g. distance between plasma and first wall, wall temperature, fusion power
 - *Control and optimisation of the plasma properties*
 - e.g. plasma shape, plasma position, plasma current, plasma density, impurity concentrations, radial distributions of plasma quantities
 - *Plasma physics studies (obtain data to be used for as basis for concept improvements)*
 - All plasma quantities
- **B) Diagnostic methods / measurement principles:**
 - *Magnetic measurements*
 - *Neutron and gamma diagnostics*
 - *Optical / IR diagnostics*
 - *Bolometric diagnostics*
 - *Spectroscopic techniques*
 - *Microwave diagnostics*
 - *Plasma-facing components and operational diagnostics*

ITER: Diagnostic Implementation Scheme

(P. Thomas, ITER)

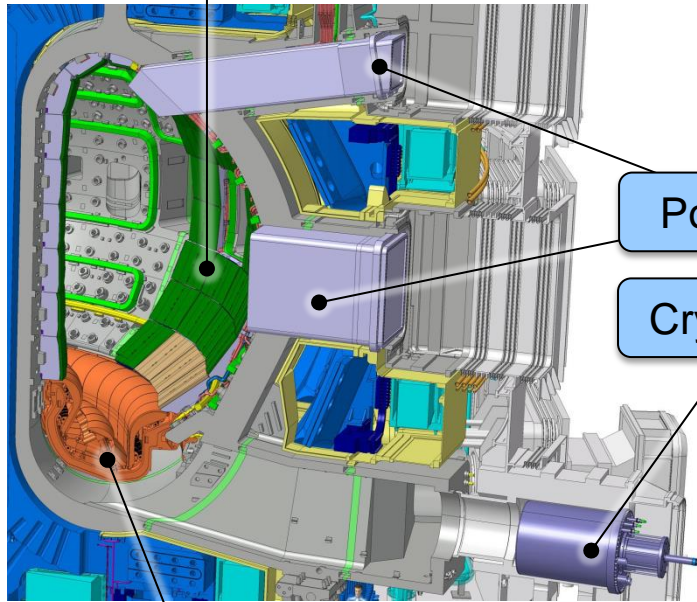


Remote Handling – ITER RH philosophy

(P. Thomas, ITER)

All of the in-vessel components must be handled and maintained using remote handling methods.

Blanket Modules

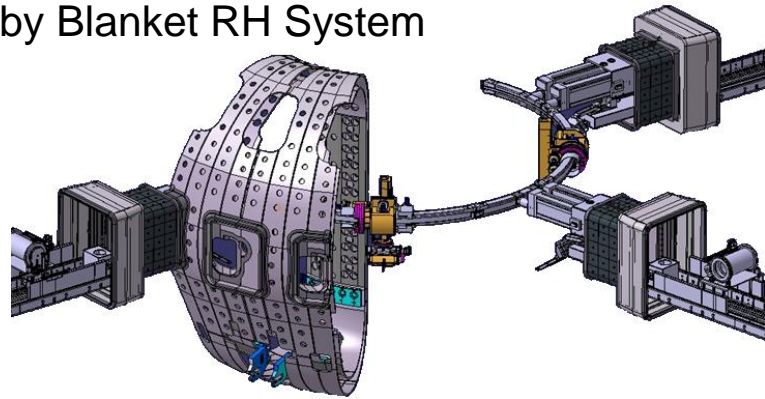


Port Plugs

Cryopumps

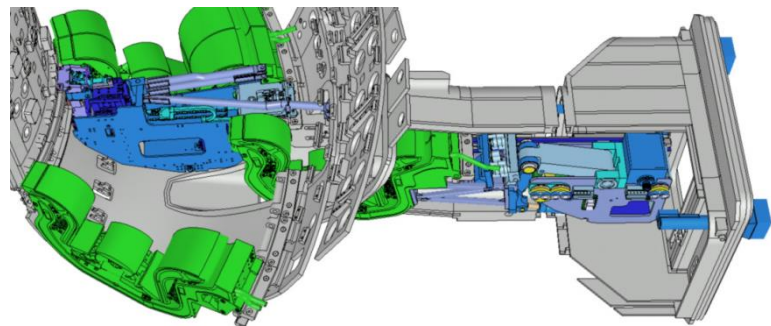
Divertor Cassettes

by Blanket RH System



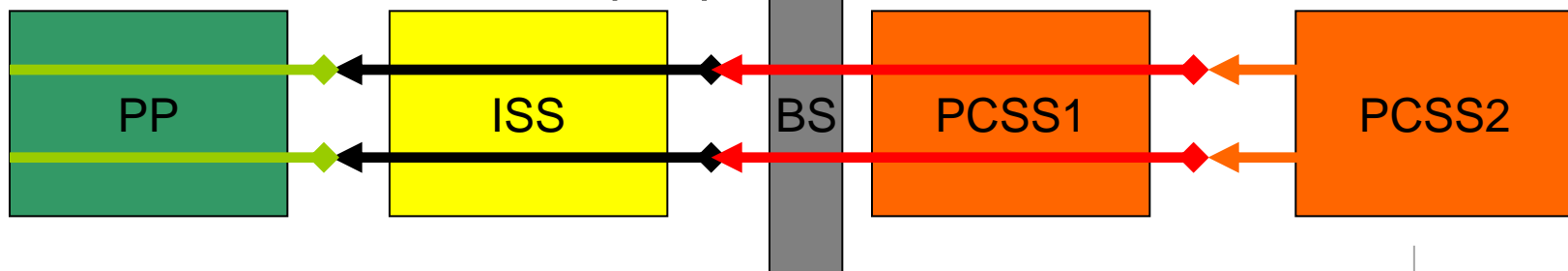
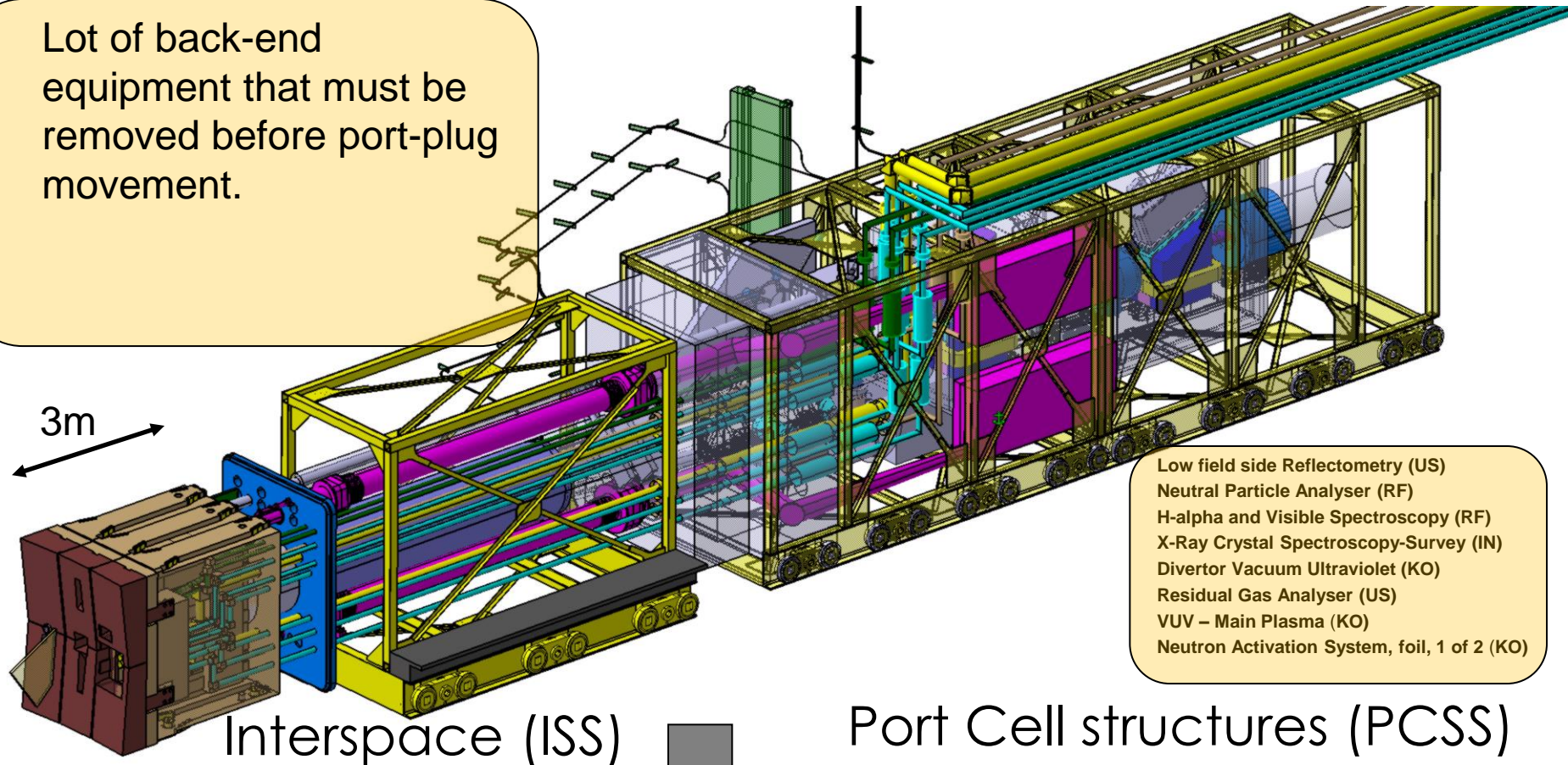
by Cask & Plug RH System
(next slide)

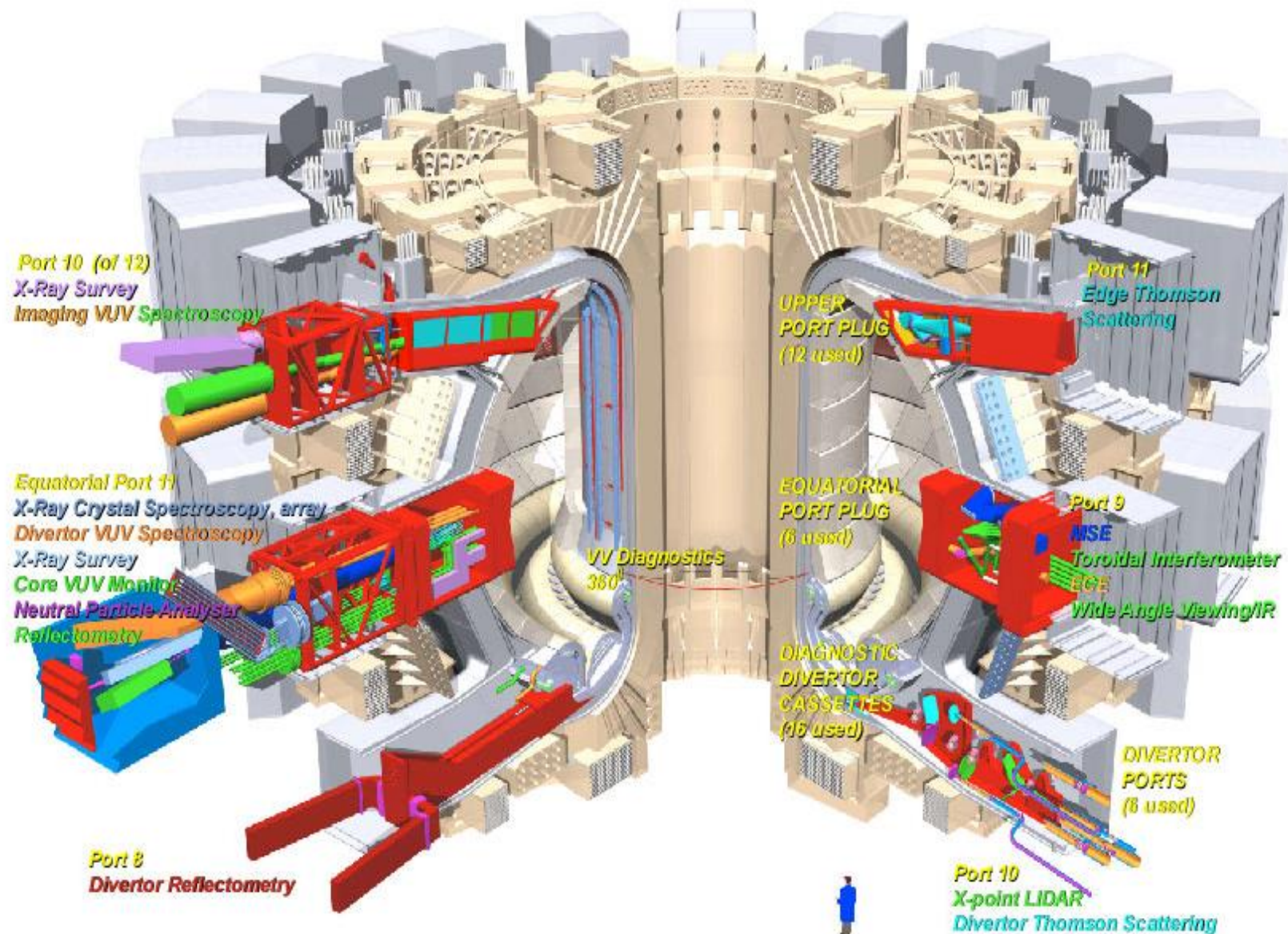
by Divertor RH System



(P. Thomas, ITER)

- Lot of back-end equipment that must be removed before port-plug movement.





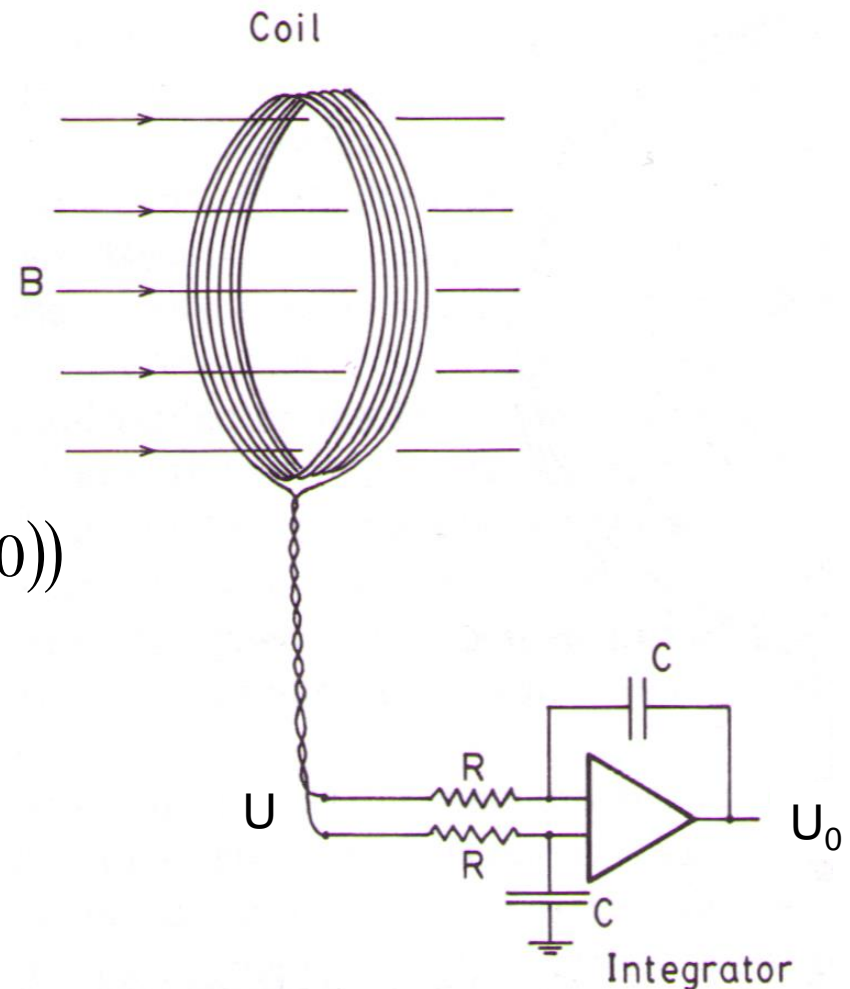
Basic principle:

A magnetic field $B(t)$ induces a voltage U in a coil with N windings and area A according to Faraday's law:

$$U = - \frac{\partial \Phi}{\partial t} = - \int_A \frac{\partial B}{\partial t} dA \approx -N A \frac{\partial B}{\partial t}$$

From the time integration of the voltage U we may derive the magnetic field $B(t)$:

$$U_0 = - \frac{N A}{R C} \int_0^t \frac{\partial B}{\partial t} dt = - \frac{N A}{R C} (B(t) - B(0))$$



Basic principle:

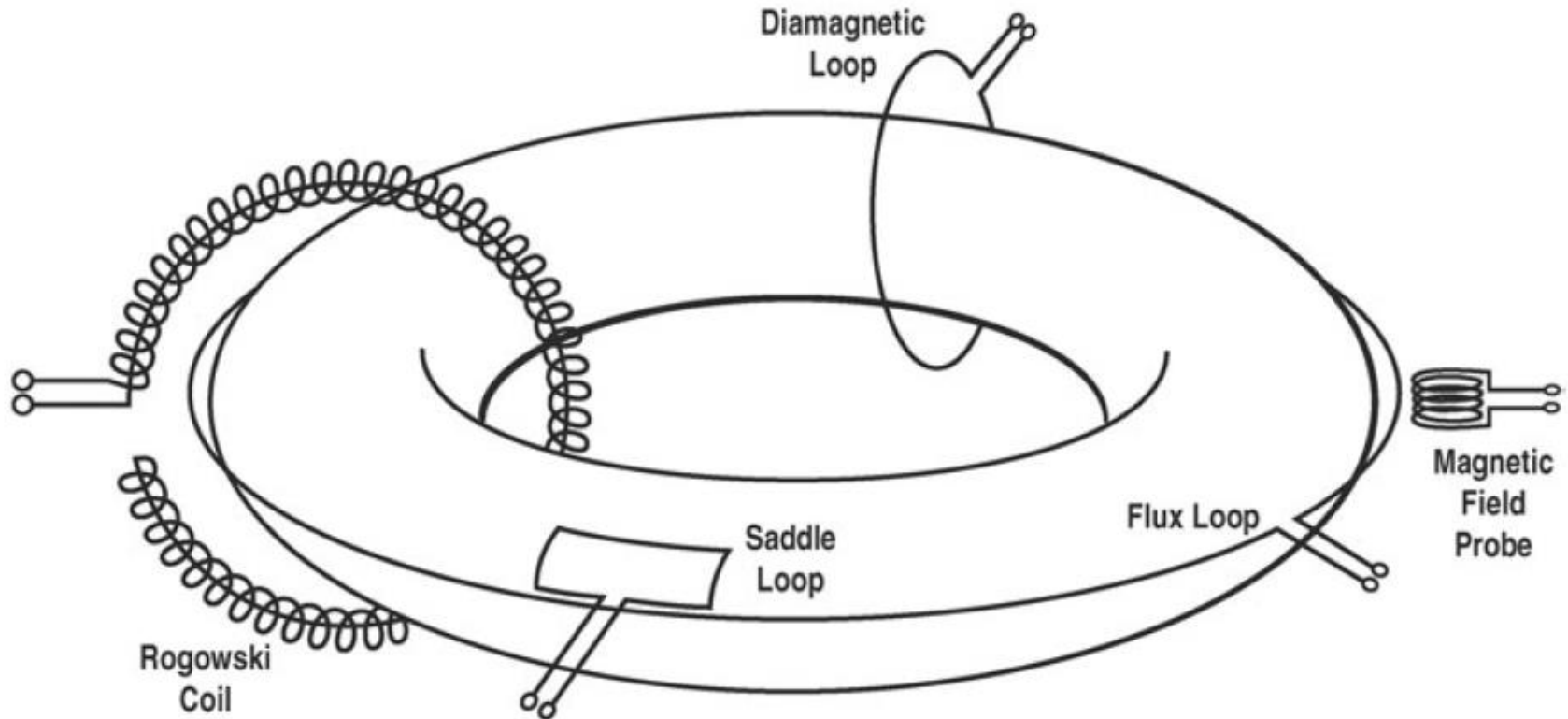
A magnetic field $B(t)$ induces a voltage U in a coil with N windings and area A according to Faraday's law:

$$U = - \frac{\partial \Phi}{\partial t} = - \int_A \frac{\partial B}{\partial t} dA \approx -N A \frac{\partial B}{\partial t} \quad (\Phi = \text{magnetic flux})$$

From the time integration of the voltage U we may derive the magnetic field $B(t)$.

Technical challenges:

- Signal is zero during phases of constant magnetic field
- Integration of signals is struggling with offset voltages in electronics or spurious voltages
- Finite size of coils \rightarrow only averaged values of B can be obtained
- Three dimensional structure of magnetic field in a tokamak: $B_t \gg B_\theta \gg B_r$, therefore a precise coil geometry is needed to separate between the field components



Strait et al., Fus. Sc. Techn. 2008

Aim:

Measurement of the plasma current

Solenoidal coil with toroidal shape, windings with uniform cross section and a number of windings per unit length n [1/m]

$$U = \dot{\psi} = n A \mu_0 \dot{I}_{Plasma}$$

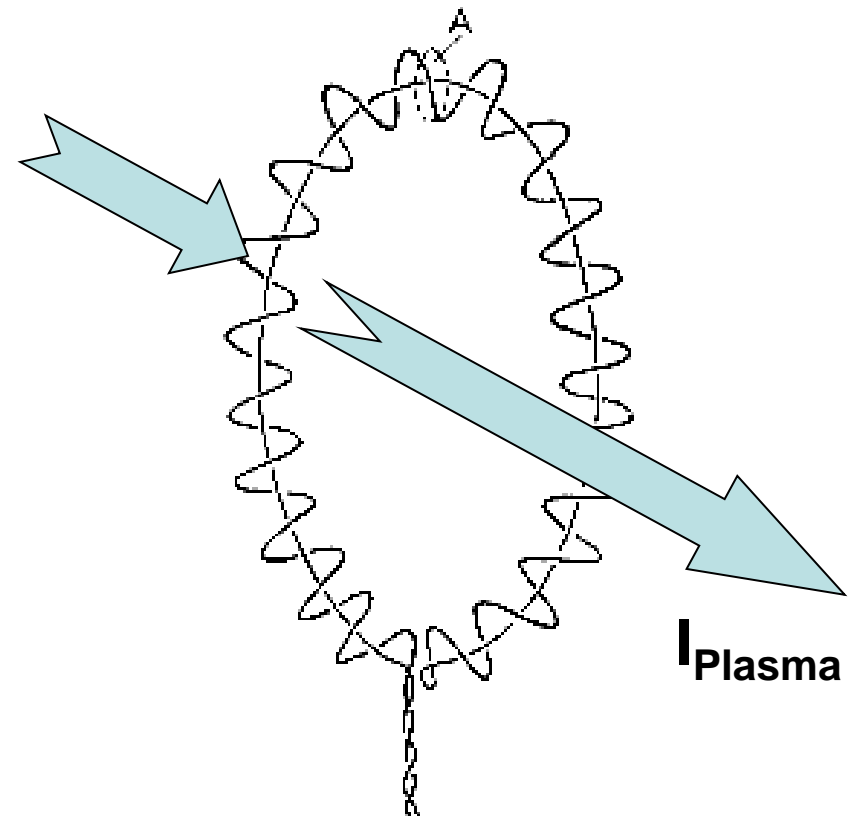
The plasma current can be obtained from the time integral of the voltage

Important:

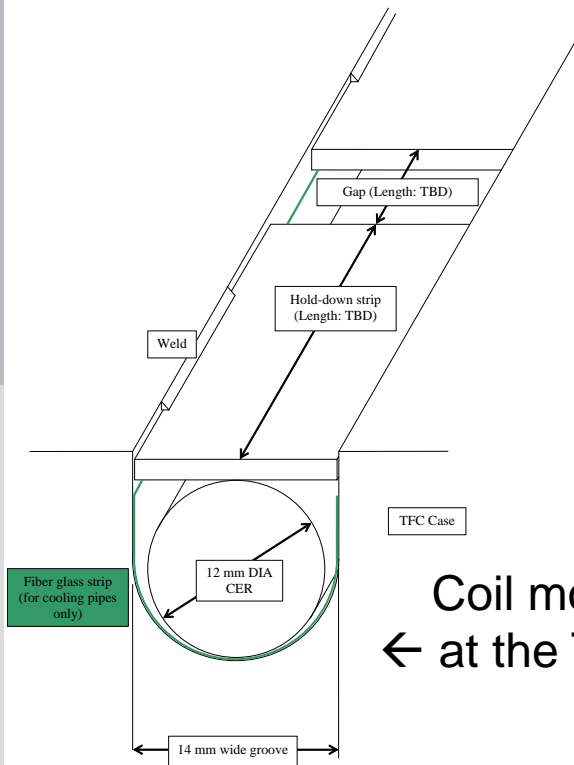
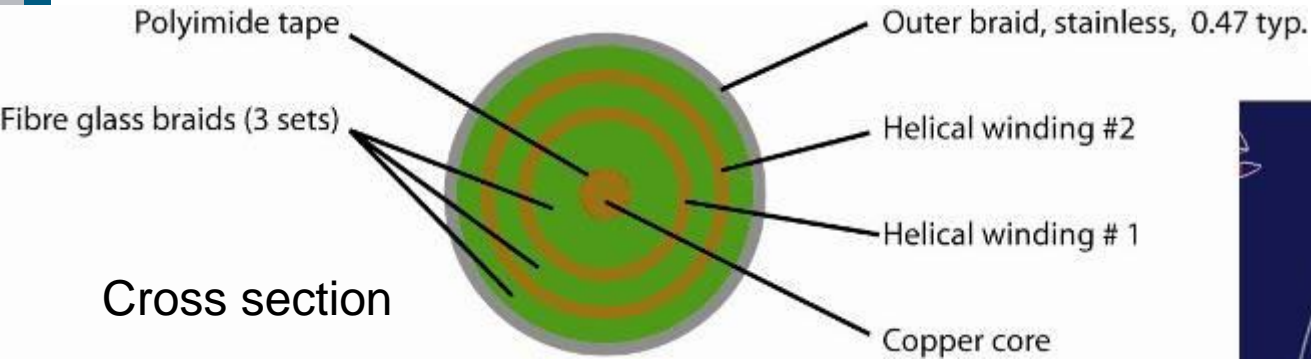
At the end of the coil the conductor is returning through the centre of the coil to the other end

→ Subtraction of toroidal flux change

From: Hutchinson, *Principles of Plasma Diagnostics*

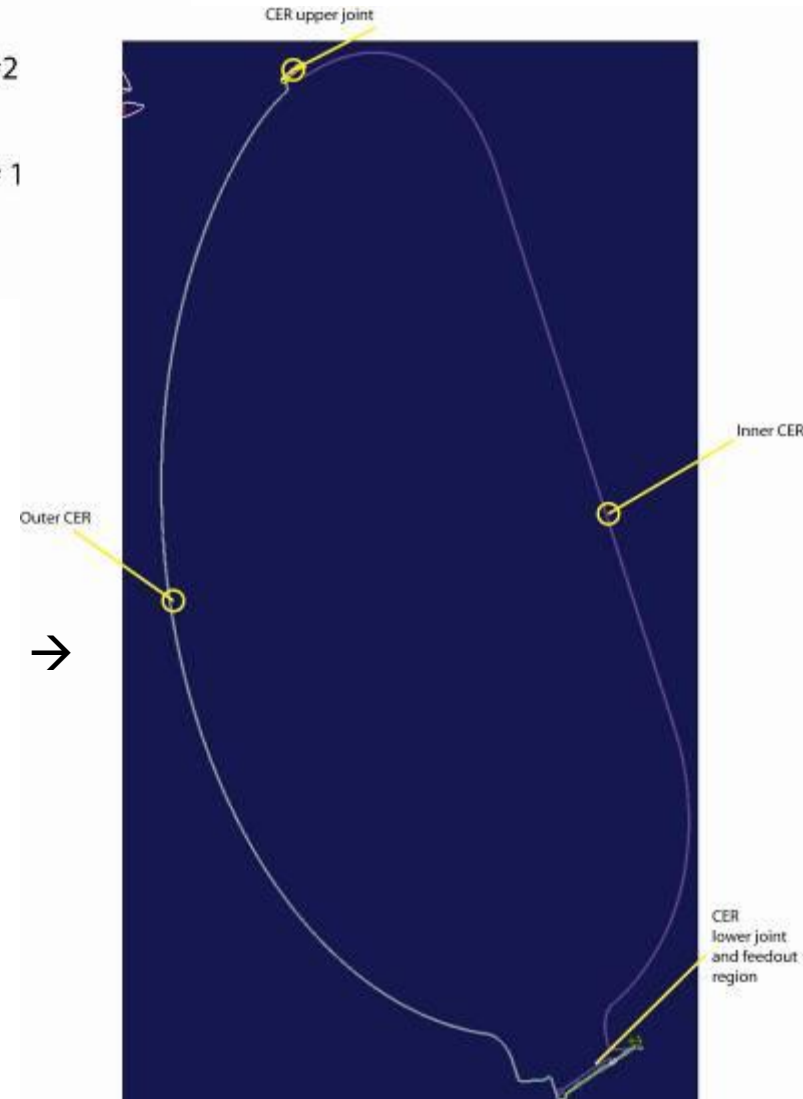


Outer ITER Rogowski coil



Coil mounted in a groove
← at the TF coil casing

Overall layout →
(2 segments)



The **plasma position** can be determined via the measurement of the fourier components of the poloidal magnetic field:

$$B_{\theta}(\theta) \approx \frac{\mu_0 I}{2\pi a} \left(1 + \frac{\Delta_H}{a} \cos \theta + \frac{\Delta_V}{a} \sin \theta \right)$$

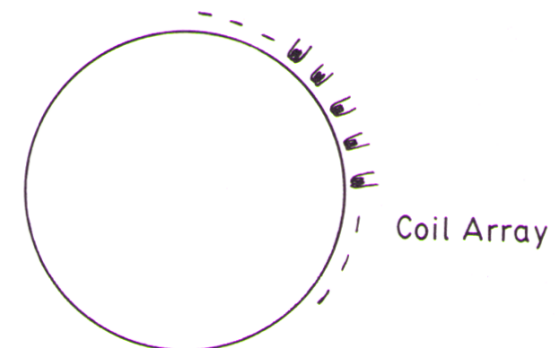
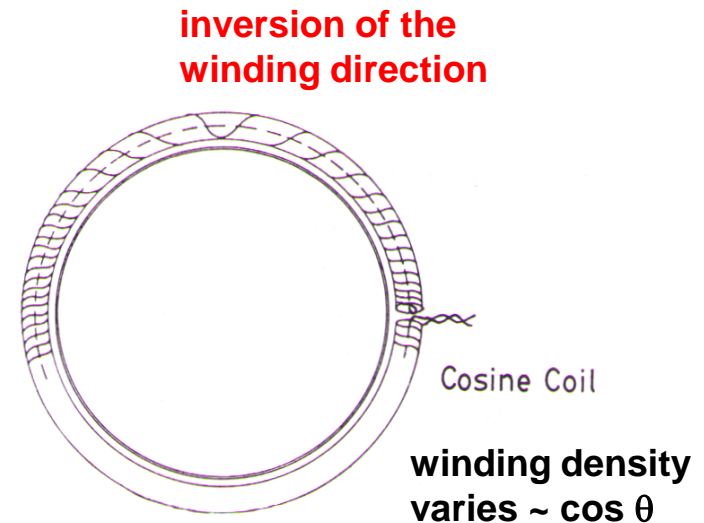
Cosine coil for horizontal position

Sine coil for vertical position (not shown)

The measured time integrated signal is proportional to the plasma dislocation Δ

Alternative approach:

Use discrete coils and perform numeric analysis for plasma position.



after: Hutchinson, *Principles of Plasma Diagnostics*

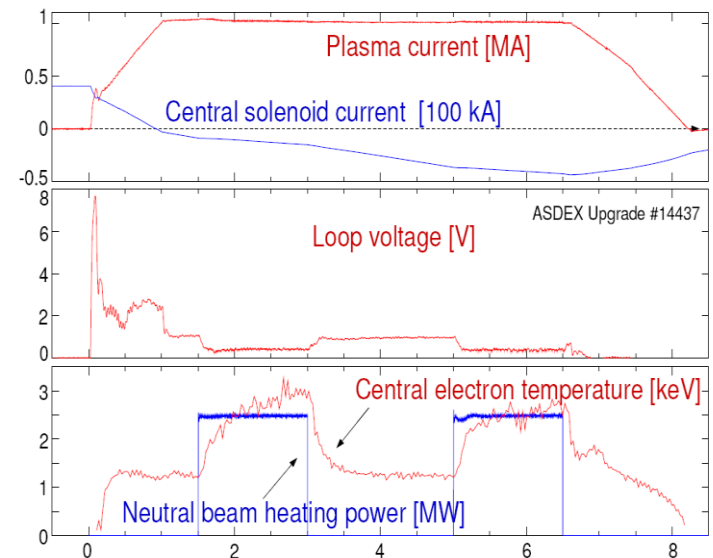
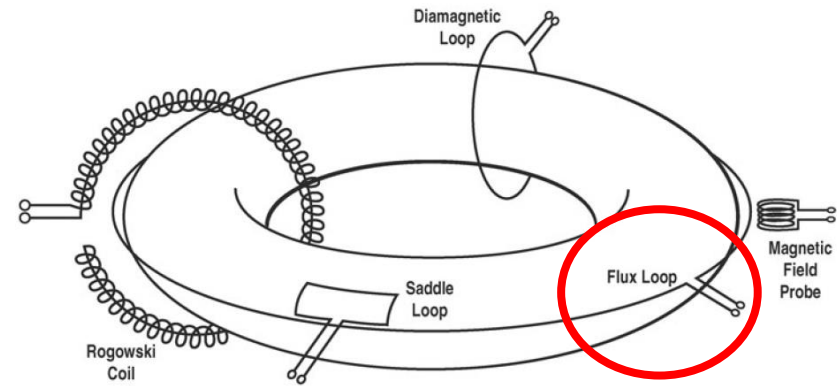
The toroidal loop voltage generated from the transformer is driving the (ohmic part of the) plasma current:

- In the stationary plasma phase, the loop voltage depends on the electrical conductivity of the plasma
- If the electron temperature T_e is known, we can derive the effective ion charge Z_{eff} from the loop voltage.

Ohmic heating power:

$$P_{\Omega} = I_p \times U_{loop}$$

$$Z_{eff} = \frac{\sum_k n_k Z_k^2}{\sum_k n_k Z_k} = \frac{\sum_k n_k Z_k^2}{n_e}$$



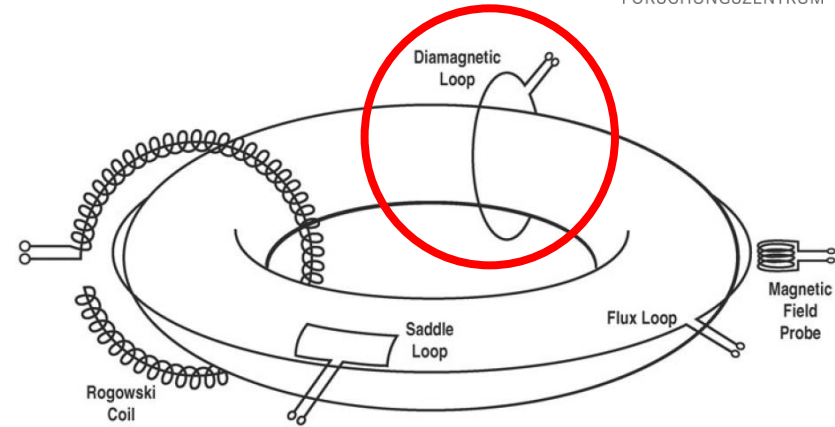
$$\langle \sigma \rangle = 1.92 \cdot 10^4 \left(2 - Z_{eff}^{-\frac{1}{3}} \right) \left(1 + \frac{5a}{R_0} + \frac{8a^2}{R_0^2} \right)^{-1} \frac{1}{Z_{eff} \ln \Lambda} \left(\frac{kT_e}{[\text{eV}]} \right)^{\frac{3}{2}} \frac{1}{[\Omega \text{ m}]}$$

Energy content of the plasma

Define the energy confinement time

$$\tau_E \equiv \frac{W_{plasma}}{P_{loss}} = \frac{V_{plasma} \frac{3}{2} \sum_k n_k k_B T_k}{P_{loss}}$$

(summation over all particle species k)



The energy confinement time can be determined from the measurement of the loss power (in the stationary case ~ heating power), the particle densities and temperatures)

In a plasma with various ion species and impurities the measurement of all densities and temperatures is a complex task.

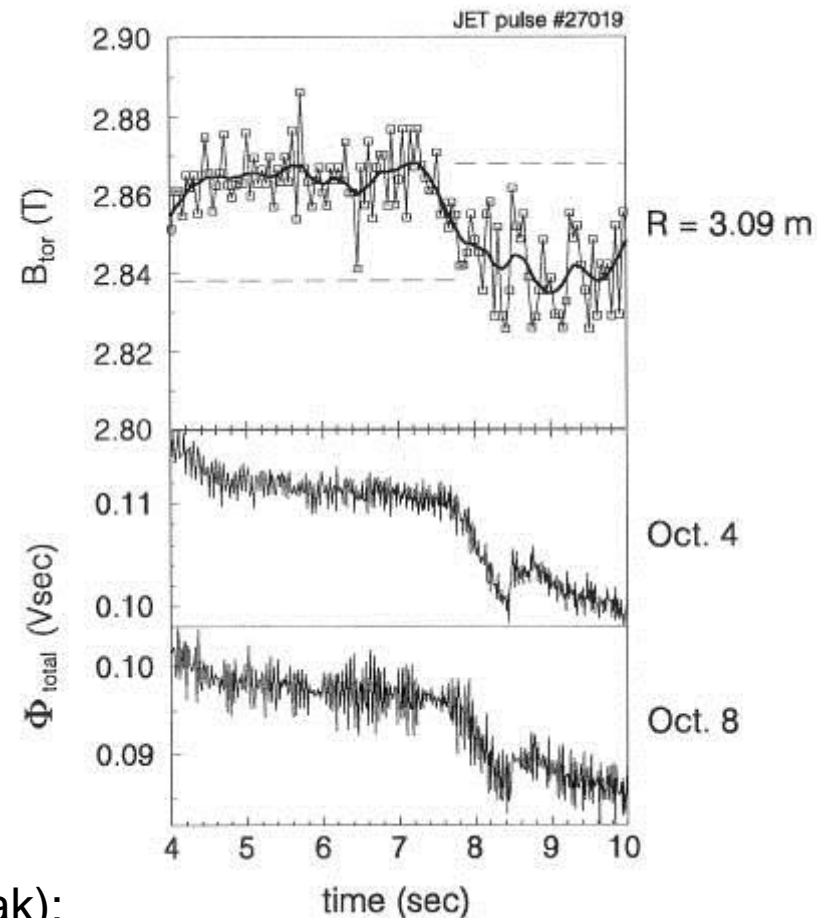
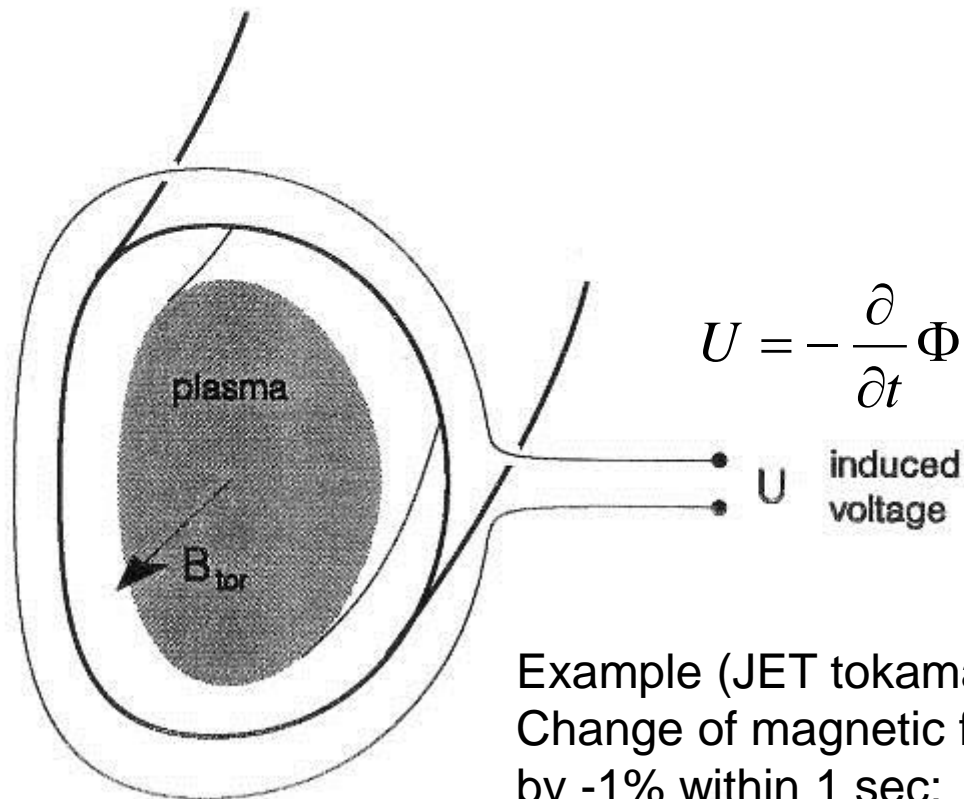
Alternatively, the kinetic plasma energy W_{Plasma} can be determined via the measurement of the change of toroidal flux:

$$W_{Plasma} = \underbrace{\frac{3}{8} \mu_0 R_0 I^2}_{\text{(inductive)}} \left(1 - \frac{8 \pi B_0}{\mu_0^2 I^2} \Delta \Phi_{tor} \right) = \underbrace{\frac{3}{8} \mu_0 R_0 I^2}_{\text{(inductive)}} - \underbrace{\frac{3 \pi B_0 R_0}{\mu_0} \Delta \Phi_{tor}}_{\text{(kinetic)}} \quad \text{(Assumption: circular plasma cross section)}$$

Diamagnetic loop

Measurement of the kinetic energy in the plasma

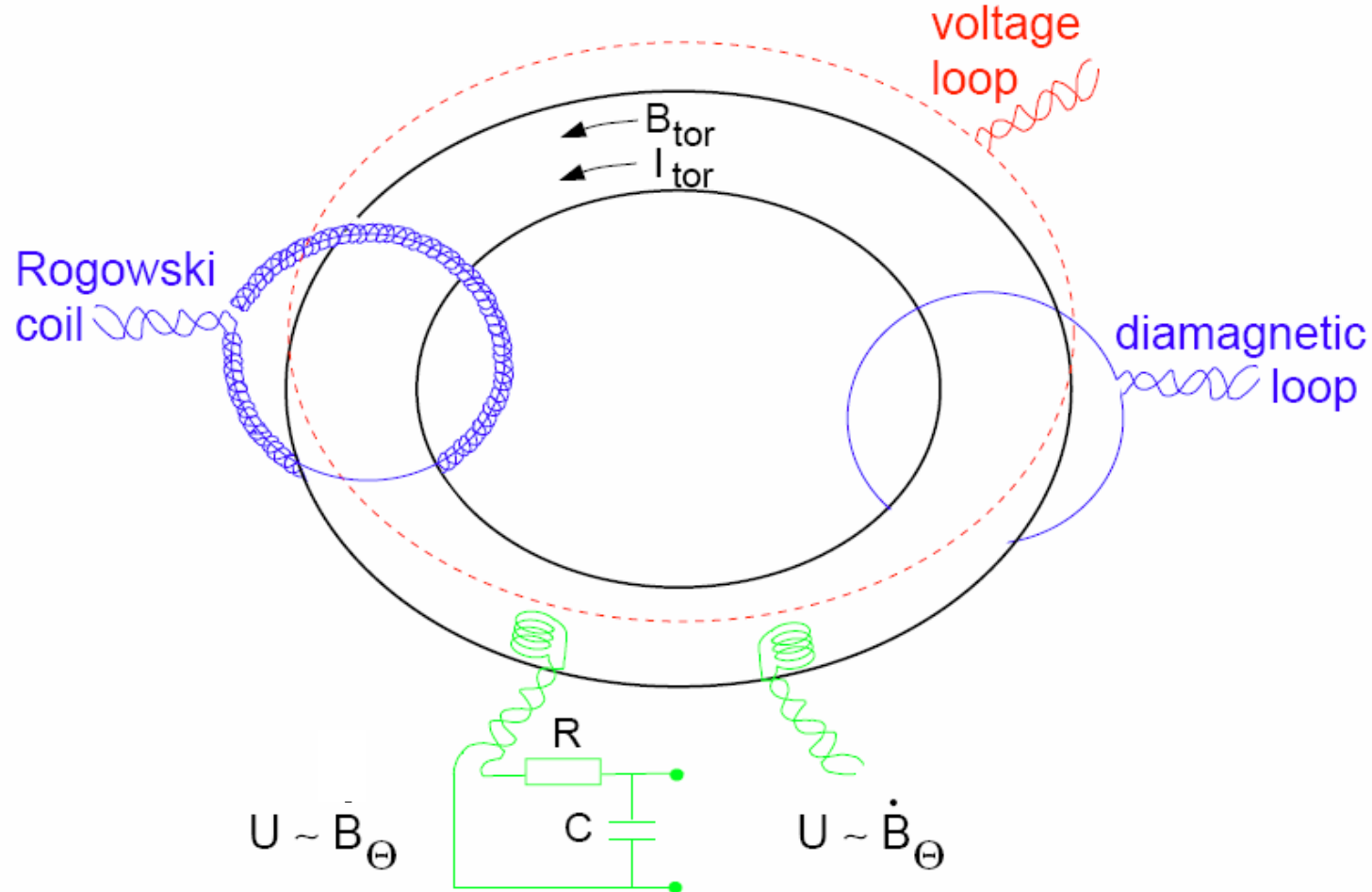
$$W_{\text{plasma}} = \underbrace{\frac{3}{8} \mu_0 R_0 I^2}_{\text{(inductive)}} - \underbrace{\frac{3 \pi B_0 R_0}{\mu_0} \Delta \Phi_{\text{tor}}}_{\text{(kinetic)}}$$



Example (JET tokamak):
 Change of magnetic field ($B_0 = 3$ T)
 by -1% within 1 sec;

$$N = 1, A = 7 \text{ m}^2 \rightarrow U = N A \text{ dB/dt} = 0.2 \text{ V}$$

Mirnov coils: measurement of magnetic field fluctuations



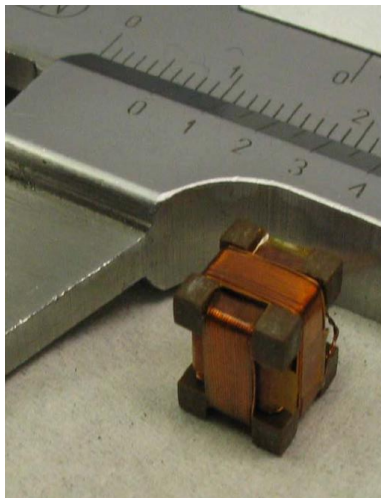
Mirnov coils are used for the local measurement of poloidal and radial magnetic field components B_θ und B_r near the plasma edge.
Problem: $B_t \gg B_\theta \gg B_r$, \rightarrow the coil geometry must be precisely aligned

Magnetic diagnostic: Mirnov coils

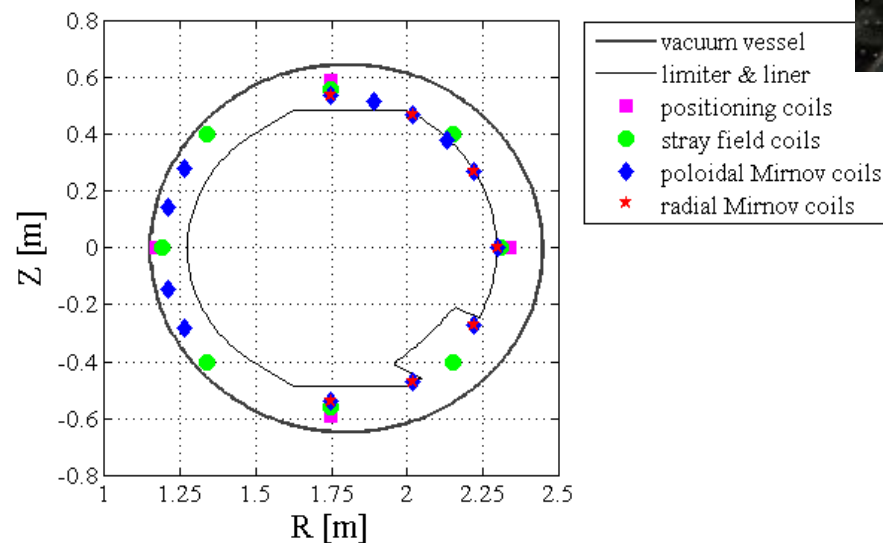
Examples for the technical realisation:



Mirnov coils on TEXTOR



Micro Mirnov coil (MAST)



Requirements for magnetic diagnostics on ITER

MEASUREMENT	PARAMETER	CONDITION	RANGE	ΔT or ΔF	ΔX or Δk	ACCURACY (2σ)
1. Plasma Current	I_p	Default	0 – 1 MA	1 ms	Integral	10 kA
			1 – 17.5 MA	1 ms	Integral	1 %
		I_p Quench	17.5 – 0 MA	0.1 ms	Integral	30 % + 10 kA
2. Plasma Position and Shape	Main plasma gaps, Δsep	$I_p > 2$ MA, full bore	-	10 ms	-	1 cm
		I_p Quench	-	10 ms	-	2 cm
	Divertor channel location (r dir.)	Default	-	10 ms	-	1 cm
		I_p Quench	-	10 ms	-	2 cm
	dZ/dt of current centroid	Default	0 – 5 m/s	1 ms	-	0.05 m/s (noise) + 2 % (error)
3. Loop Voltage	V_{loop}	Default	0 – 30 V	1 ms	4 locations	5 mV
		I_p Quench	0 – 500 V	1 ms	4 locations	10 % + 5 mV
4. Plasma Energy	β_p	Default	0.01 – 3	1 ms	Integral	5 % at $\beta_p=1$
		I_p Quench	0.01 – 3	1 ms	Integral	~ 30%
8. Locked Modes	$B_r(mode) / B_p$		$10^{-4} - 10^{-2}$	1 ms	(m,n) = (2,1)	30 %
9. Low (m,n) MHD Modes, Sawteeth, Disruption Precursors	Mode complex amplitude at wall		TBD	DC – 3 kHz	(0,0) < (m,n) < (10,2)	10 %
21. Halo Currents	Poloidal current	In disruption	0 – 0.2 I_p	1 ms	9 sectors	20 %
22. Toroidal Magnetic Field	B_T		2 – 5.5 T	1 s	2 locations x 2 methods	0.1 %
27. High Frequency Macro Instabilities (Fishbones, TAEs)	Fishbone-induced perturbations in B,T,n		TBD	0.1 – 10 kHz	(m,n) = (1,1)	–
	TAE mode – induced perturbations in B,T,n		TBD	30 – 300 kHz	n = 10 - 50	–

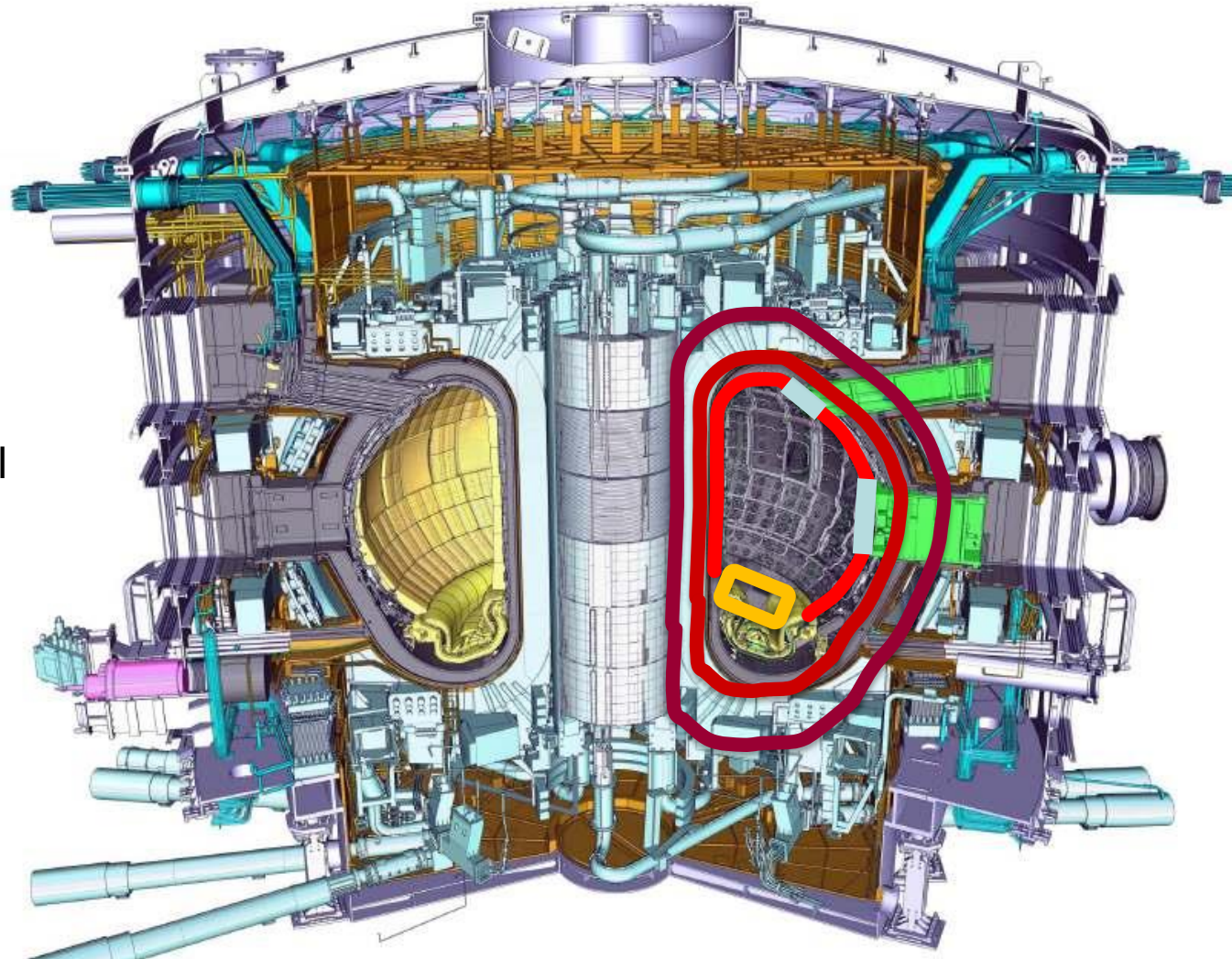
(after G. Vayakis, ITER organisation)

Effect	Symbol	Explanation
Radiation-induced conductivity	RIC	Electrical conductivity increases due to the excitation of electrons into the conduction band.
Radiation-induced electrical degradation	RIED	Electrical conductivity increases due to radiation and electric field enhanced defect aggregation.
Thermal conductivity decrease	–	Thermal conductivity decreases leading to temperature increases.
Volume changes	–	Materials swell , or in some cases shrink
Radiation-Induced Electromotive Force	RIEMF	Nuclear reactions in the sensor materials induce net current in the sensor circuit
Thermoelectric Electromotive Force	TIEMF	Parasitic thermocouple action driven by nuclear-heating
Radiation-induced thermoelectric sensitivity	RITES	Additional parasitic thermocouples generated by non-uniform material damage and transmutation
Radiation-enhanced diffusion	–	Enhanced diffusion occurs in insulating materials due to the possible existence of different charge states for defects and impurities.
Radiation-induced absorption	RIA	Optical absorption increases due to the production of defect related absorption bands, leading to light transmission loss.
Radioluminescence or radiation-induced emission	RL or RIE	Light emission due to excitation of defects and impurities.

Where are magnetics mounted?

(G. Vayakis, ITER)

- On the divertor (most exposed)
- Just behind the ITER blanket in vessel
- On the outer vessel skin
- Inside the TF coil (least exposed)



Note: backward mounting results in longer lifetime of components but reduced performance due to signal attenuation and shielding by eddy currents

Most basic case: cold plasma without magnetic field

(ω = angular frequency; N = refractive index)

$$\omega^2 - \omega_P^2 = k^2 c^2; \quad N = \sqrt{1 - \left(\frac{\omega_P}{\omega}\right)^2}$$

where the plasma frequency is given by

$$\omega_P = \sqrt{n_e \frac{e^2}{\epsilon_0 m_e}} \quad \text{(this is the oscillation frequency of the electron fluid if the electrons are displaced against the ion background)}$$

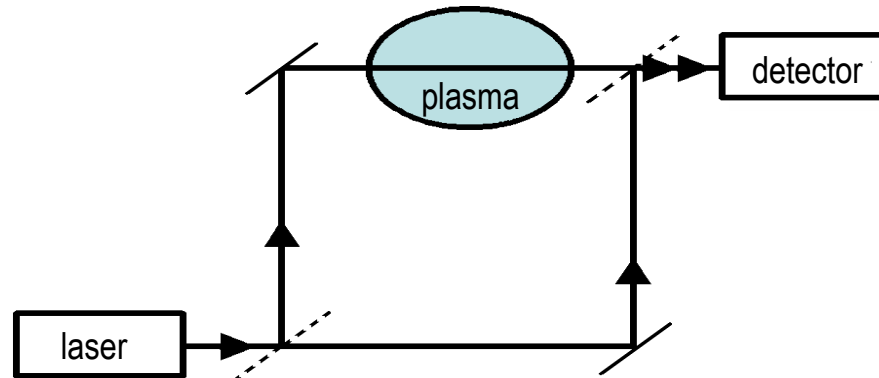
In this most basic case any electromagnetic wave with frequency below the plasma frequency cannot penetrate into the plasma \rightarrow the wave will be reflected \rightarrow „reflectometry“

Example:

For an electron density $n_e = 10^{20} \text{m}^{-3}$ we obtain $\omega_P = 5.6 \times 10^{11} \text{s}^{-1}$, $f = \omega_P / 2\pi = 90 \text{ GHz}$
this translates to a wavelength of $\lambda = c / f = 3.34 \text{ mm}$ (microwave range)

Wave with frequencies above the plasma frequency can penetrate into the plasma, but they experience a phase shift ($N < 1$).

Interferometry: measurement of electron density integrated along the sightline

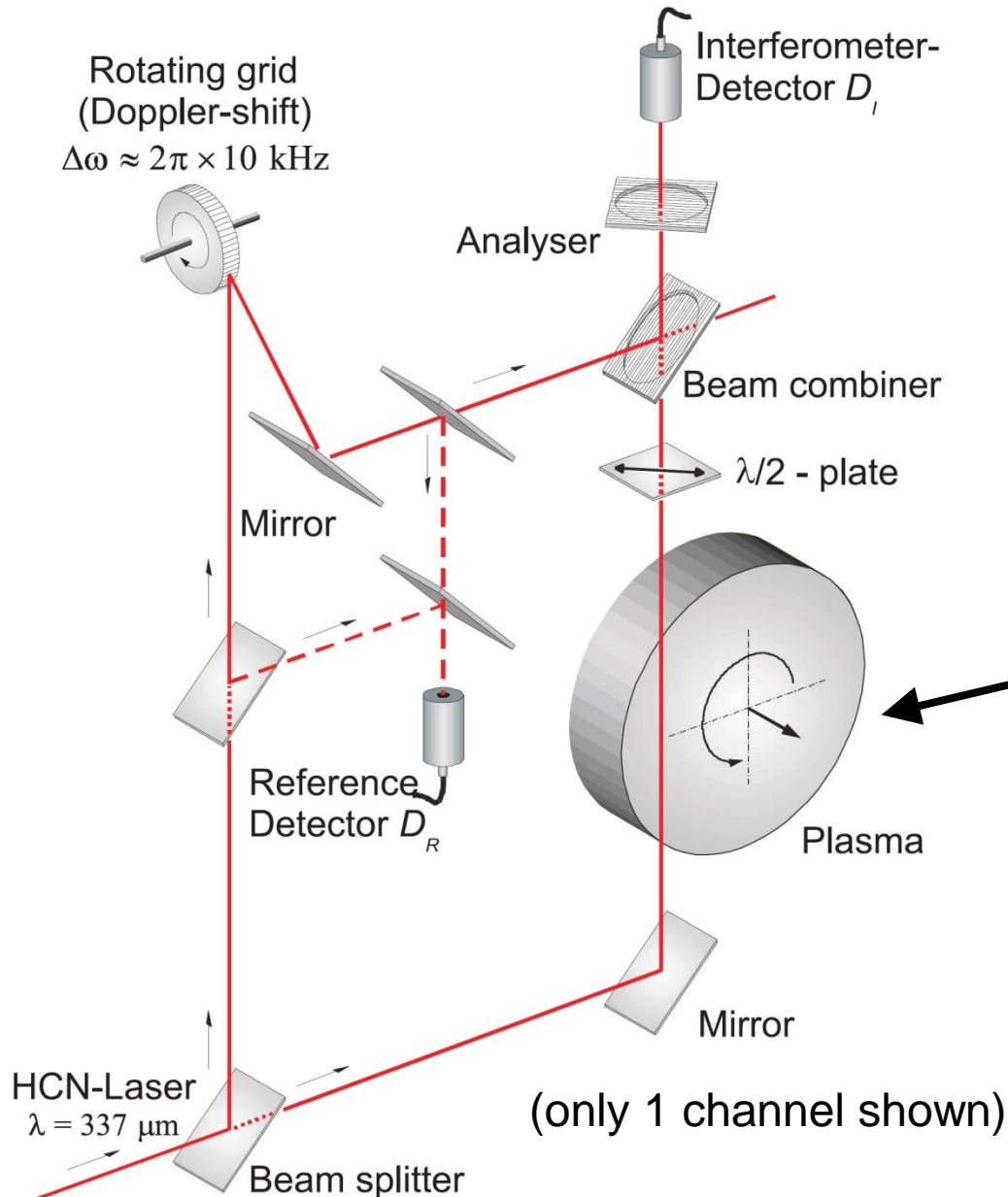


- The refractive index N of a plasma depends on the electron density and on the wavelength
- The interferometer measures the phase shift due to the plasma (phase angle ϕ)

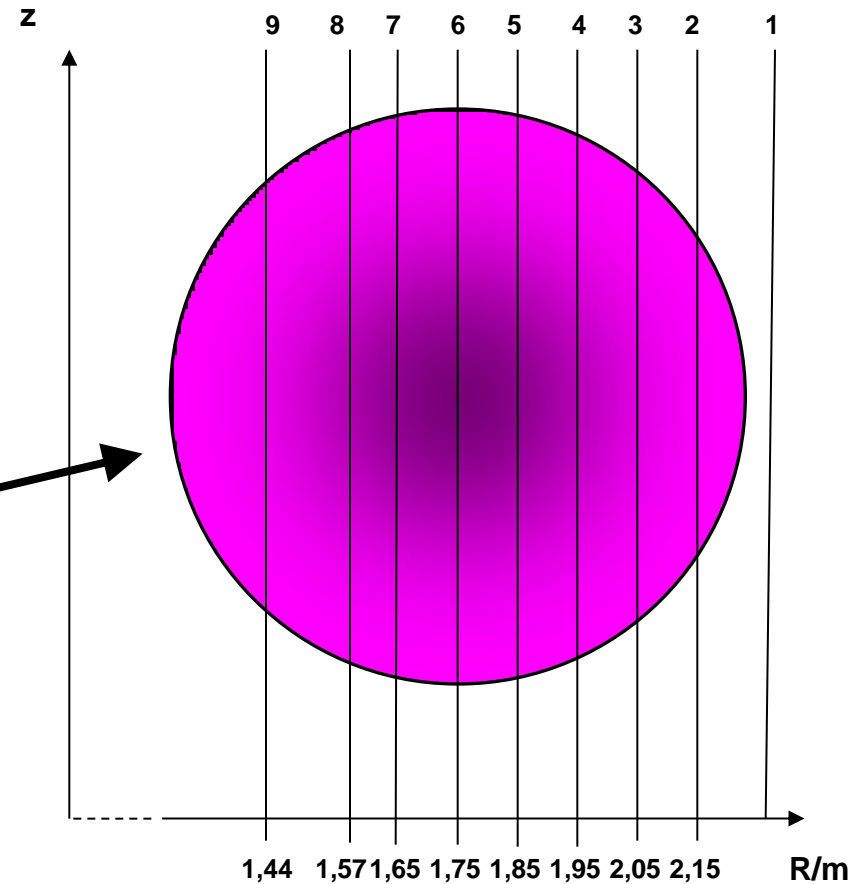
$$N = \sqrt{1 - \left(\frac{\omega_P}{\omega}\right)^2}, \quad \omega_P = \sqrt{n_e \frac{e^2}{\epsilon_0 m_e}}$$

$$\phi = \frac{e^2}{4\pi\epsilon_0 c^2 m_e} \lambda \int n \, dl$$

HCN interferometer on TEXTOR



arrangement of 9 channels



Propagation of a laser beam in a plasma with electron density n_e and a magnetic field component $B_{||}$ oriented along the beam

→ rotation the beam polarisation (= Faraday rotation):

$$\Delta\theta = 2.62 \times 10^{-13} \lambda^2 \int_{Z_0}^{Z_1} n_e B_{||} dZ$$

Z = coordinate along $B_{||}$

λ = laser wavelength [m]

n_e = electron density [m^{-3}]

$B_{||}$ = magnetic field component along the beam [T]

Example: $\lambda = 10 \mu\text{m}$, $Z_1 - Z_0 = 10 \text{ m}$, $B_{||} = 5 \text{ T}$, $n_e = 10^{20} \text{ m}^{-3} \rightarrow \Delta\theta = 0.113$

Current density measurement in a tokamak via polarimetry

H. Soltwisch, Rev. Sci. Instrum. 1986

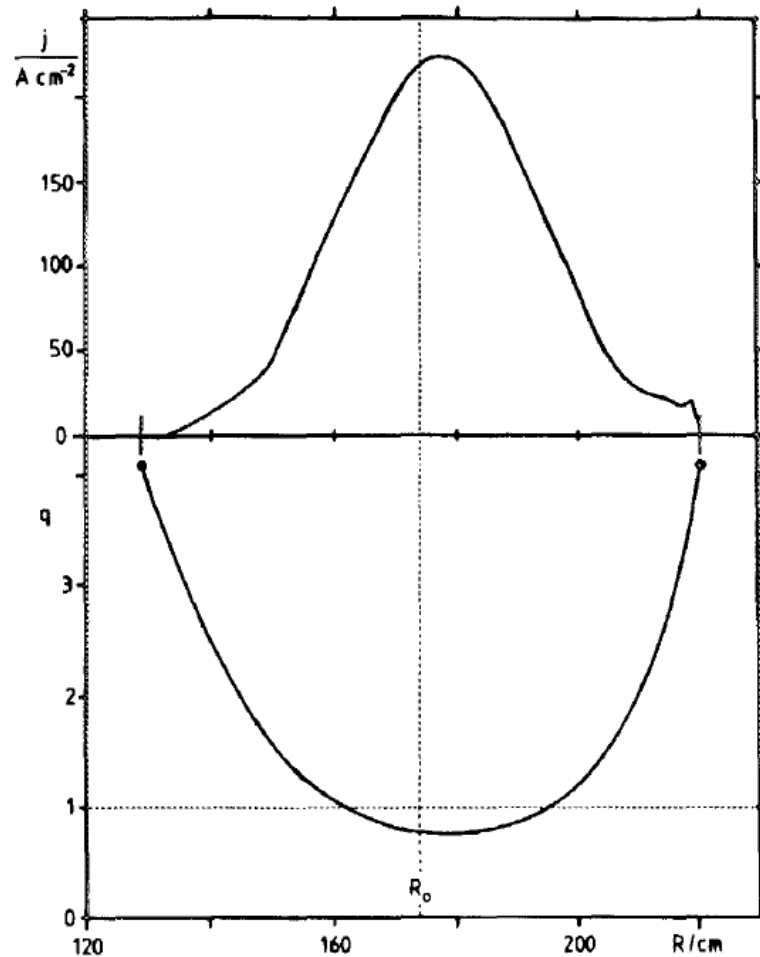
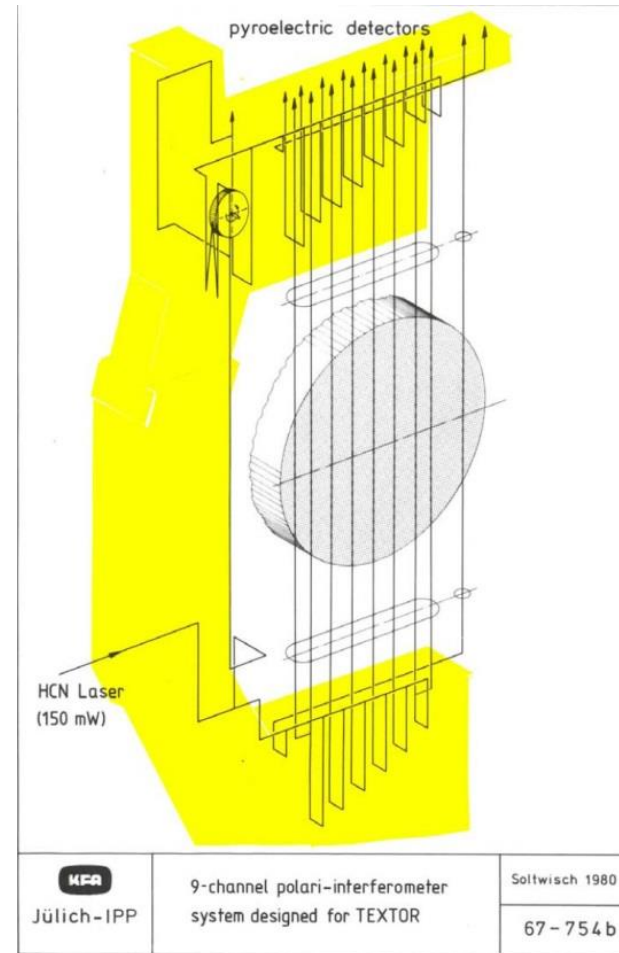


FIG. 8. Current density (upper trace) and safety factor (lower trace) vs major radius as derived from the data shown in Fig. 4 at $t = 1$ s.



The current density in a tokamak is stronger peaked than expected $\rightarrow q < 1$ in the plasma centre possible

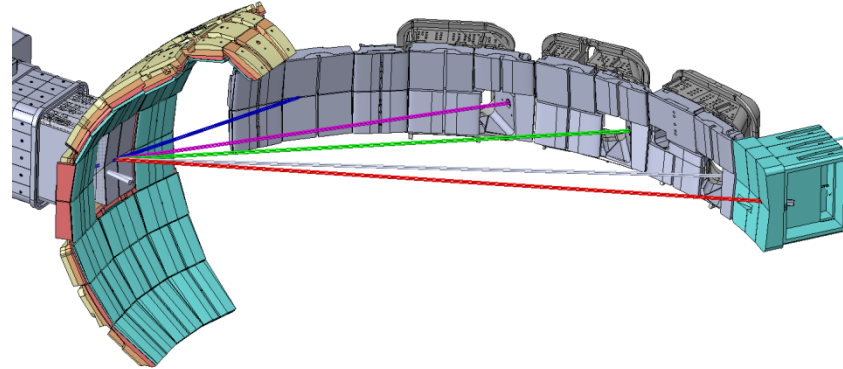
Interferometer:

max. phase: ~ 10 fringes

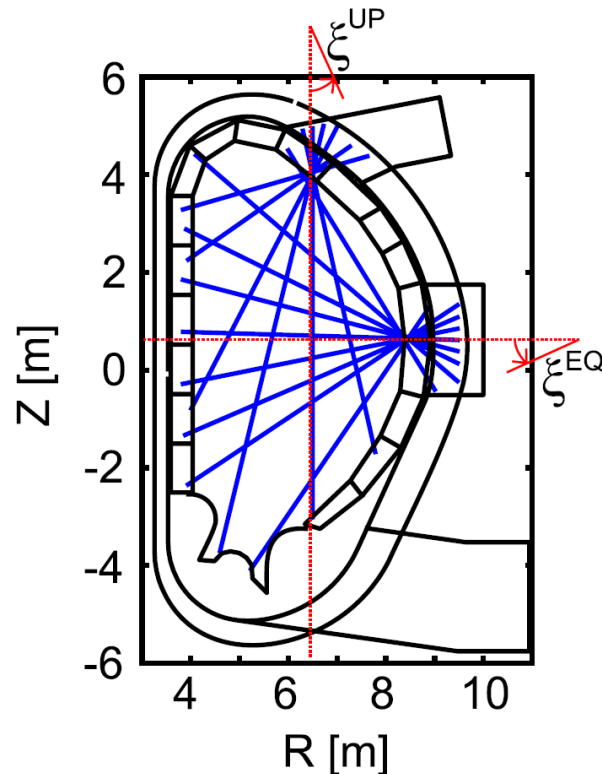
polarimetry

max. phase: $\ll 1$ fringe

V.V. Mirnov et al.
Varennia Conf. 2013



(M. A. van Zeeland, *Rev. Sci. Instrum.*, 2013)



Polarimetry data analysis has to take into account:

- Faraday effect (**B** || beam)
- Cotton-Mouton (C-M) effect (**B** \perp beam)
- Temperature dependence of rotation angle and relativistic effects

Measurement of electron cyclotron emission (ECE) to determine the electron temperature

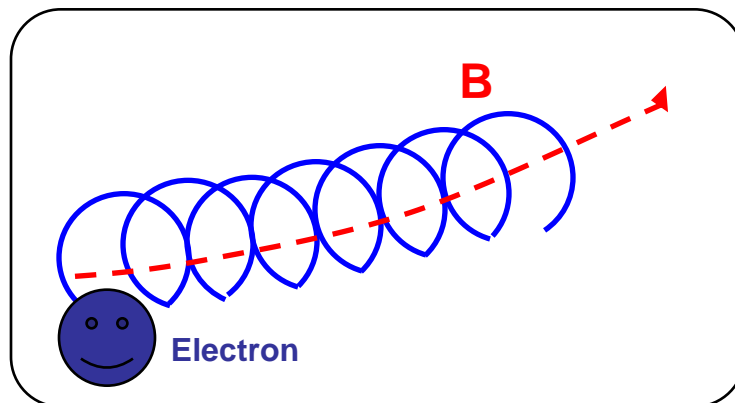
Electrons and ions gyrate around the magnetic field lines → centrifugal forces

Classical electrodynamics:

Accelerated charged particles emit electromagnetic radiation

The frequency of the ECE radiation is the gyration frequency ω_{ce} (and in principle also ω_{ci}) and their higher harmonics $n\omega_{ce}$ (and $n\omega_{ci}$), with $n = 2, 3, \dots$

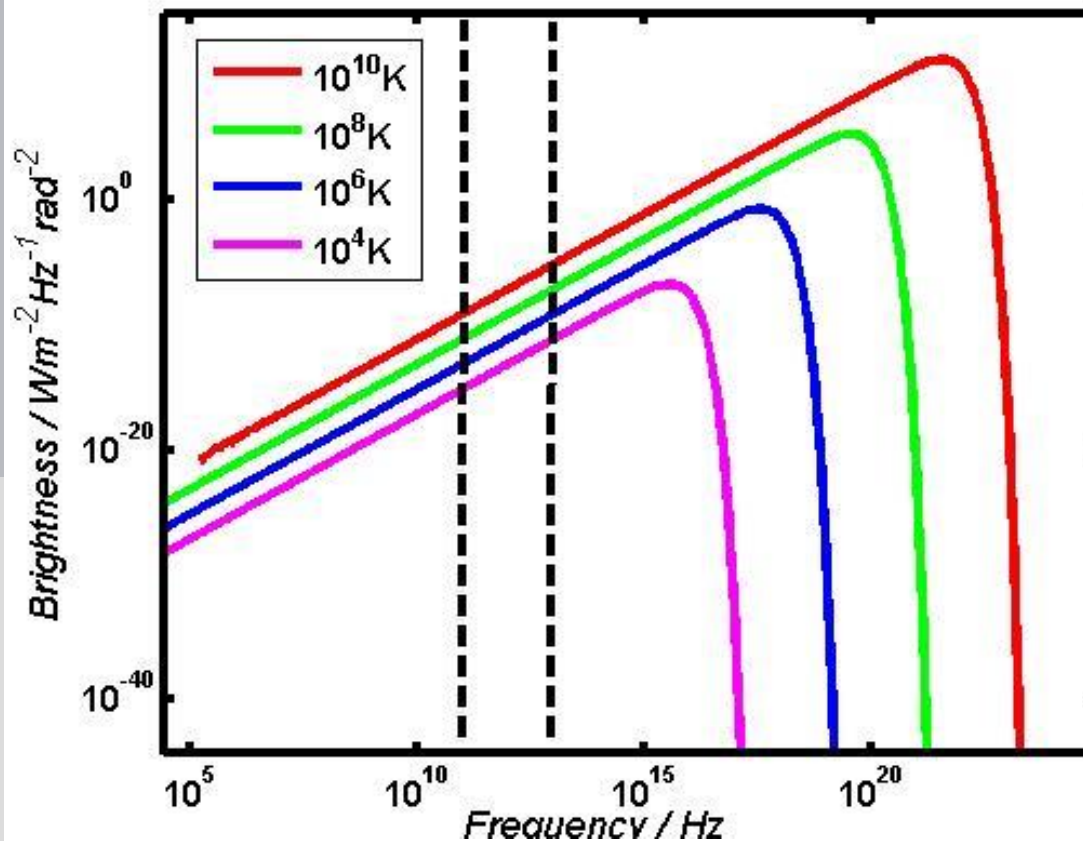
In a fusion plasma the radiation at the fundament frequency ω_{ce} is **optically thick**.
The emitted photons will be absorbed and re-emitted several times in the plasma.
→ ECE is black-body radiation



$$\omega_{ce} = \frac{eB}{m_e}$$

Determination of the electron temperature T_e from ECE measurements

Optically thick radiation can be described by a **Planck curve**:



$$B(\omega) = \frac{\hbar \omega^3}{8\pi^3 c^2} \left(\frac{1}{\exp\left(\frac{\hbar \omega}{k_B T_e}\right) - 1} \right)$$

The electron temperature can be determined from an intensity measurement

Analysis of ECE measurements

In a fusion plasma with magnetic field the gyrating electrons radiate at the cyclotron frequency $\omega_{ce} = eB/m_e$ and at their higher harmonics.

Apply the **low frequency approximation**: $e^{-\frac{\hbar\omega}{kT}} - 1 \approx \frac{\hbar\omega}{kT}$

In this case the **Planck curve**

$$B(\omega) = \frac{\hbar\omega^3}{8\pi^3c^2} \left(\frac{1}{\exp\left(\frac{\hbar\omega}{k_B T_e}\right) - 1} \right)$$

simplifies towards the **Rayleigh-Jeans law**:

$$B(\omega) = \frac{\omega^2 k_B T_e}{8\pi^3 c^2}$$

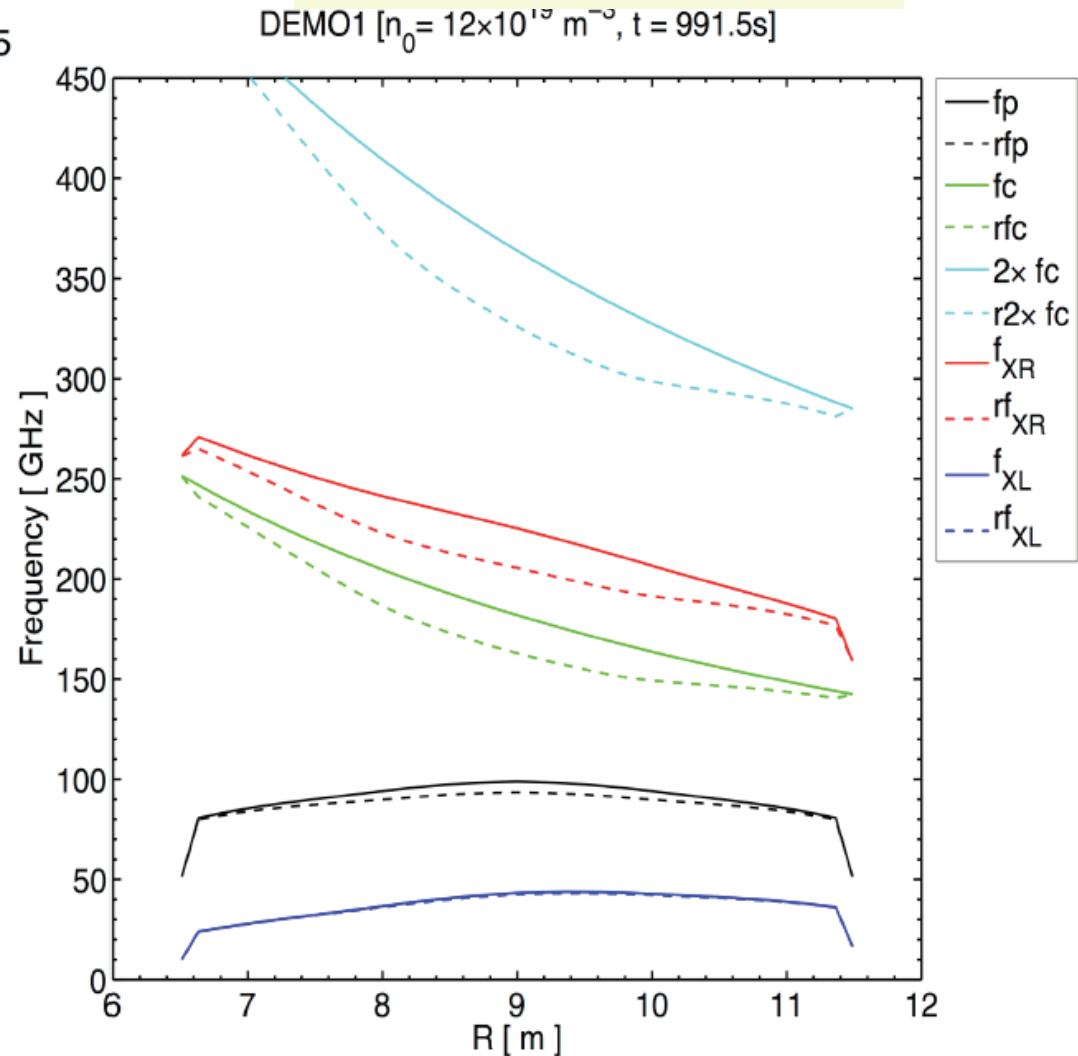
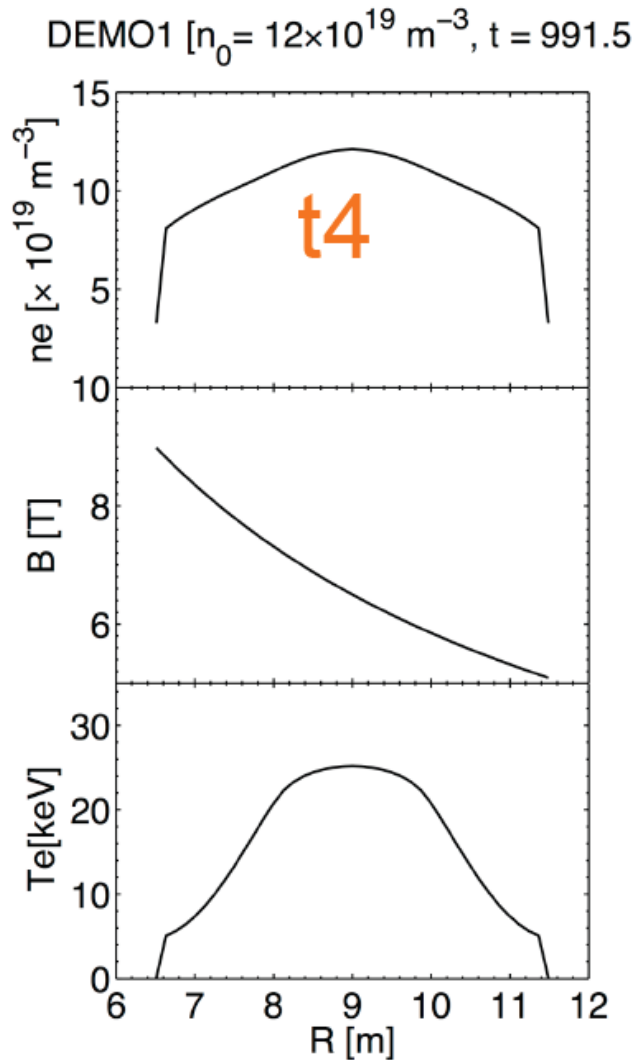
The measured ECE intensity is proportional to the electron temperature.

The ECE diagnostic needs an intensity calibration.

Radial dependence of frequencies for microwave diagnostics on a DEMO reactor

(A. Silva et al.)

$$B(R) = \frac{B_0 R_0}{R} ; \quad \omega_{ce} = \frac{eB}{m_e}$$



1. Relativistic correction: For high electron temperatures, the relativistic dependence of the mass has to be considered:

$$\omega_{ce} = \frac{eB}{m_e \gamma} \quad \gamma = \sqrt{\frac{1}{1 - \frac{v^2}{c^2}}} > 1$$

- For a given frequency, the **actual place of measurement is shifting towards the high field side of the torus**, i.e. to lower values of R

2. Diamagnetic correction: The sum of kinetic plasma pressure and magnetic pressure is constant:

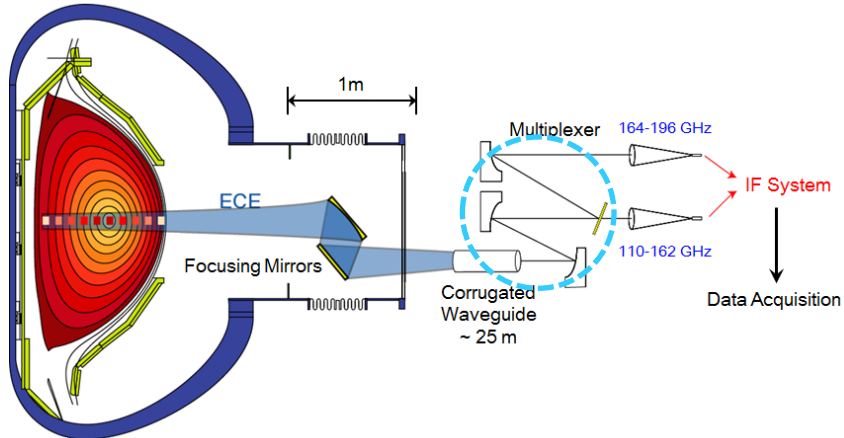
$$p + \frac{B^2}{2\mu_0} = \text{const} = \frac{B_0^2}{2\mu_0}$$

- Again, for a given frequency, the **actual place of measurement is shifting towards the high field side of the torus**, i.e. to lower values of R

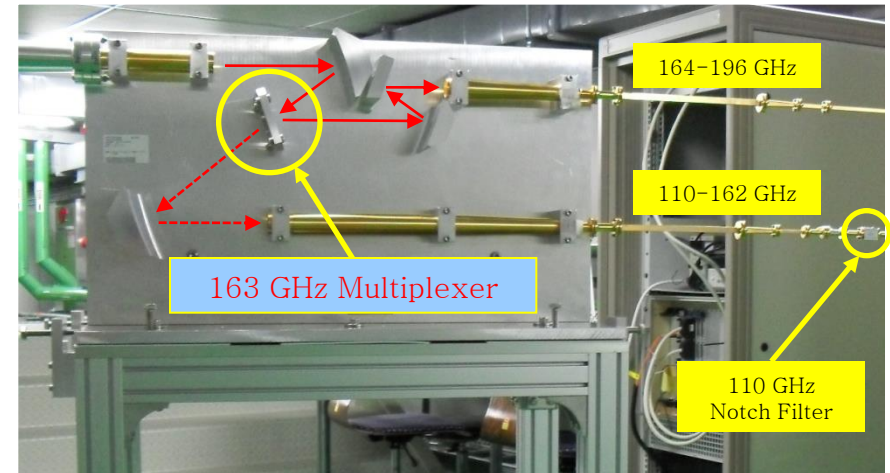
KSTAR ECE System : 110-196 GHz

K. D. Lee and Seong-Heon Seo, NFRI (Korea)

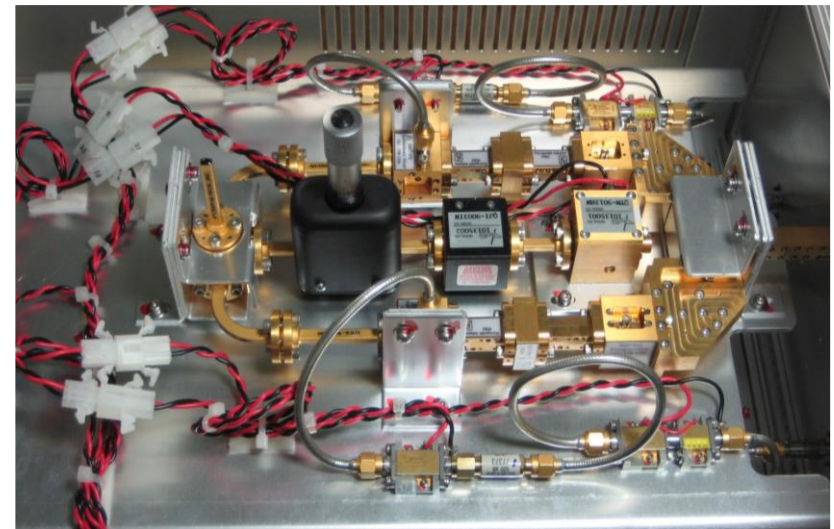
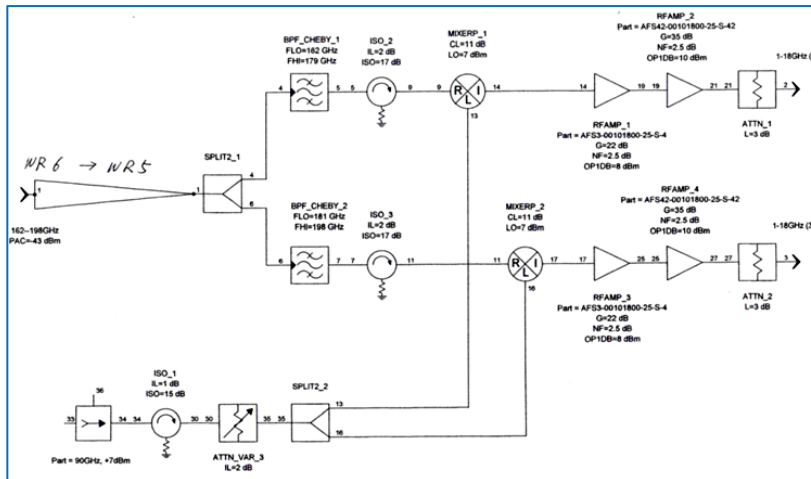
Schematic of KSTAR ECE System



• Multiplexer Optics (2010-2012)

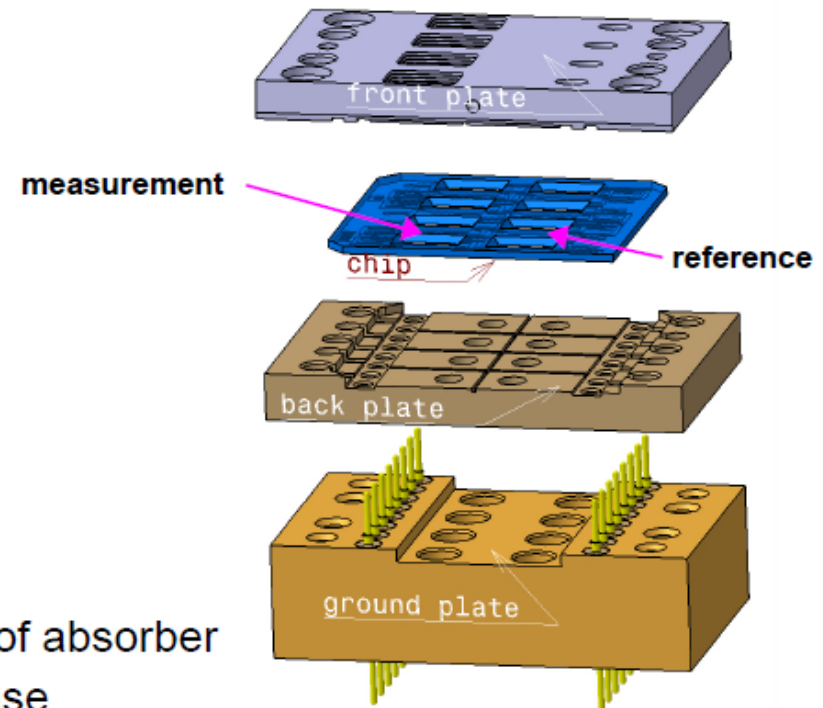
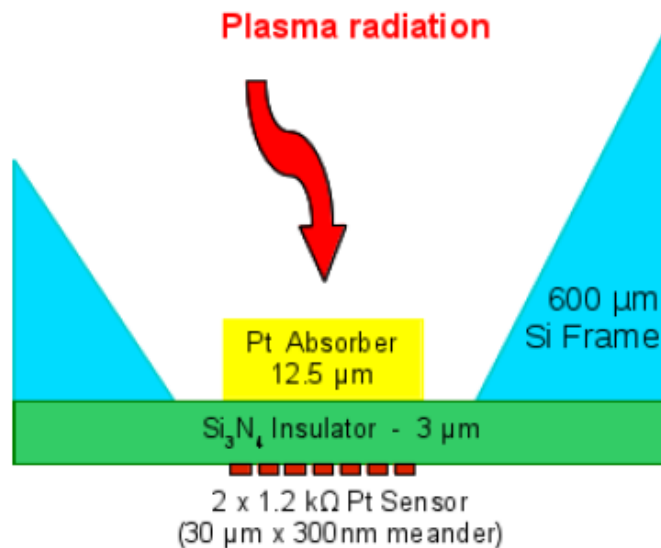


Overview of ECE Radiometer



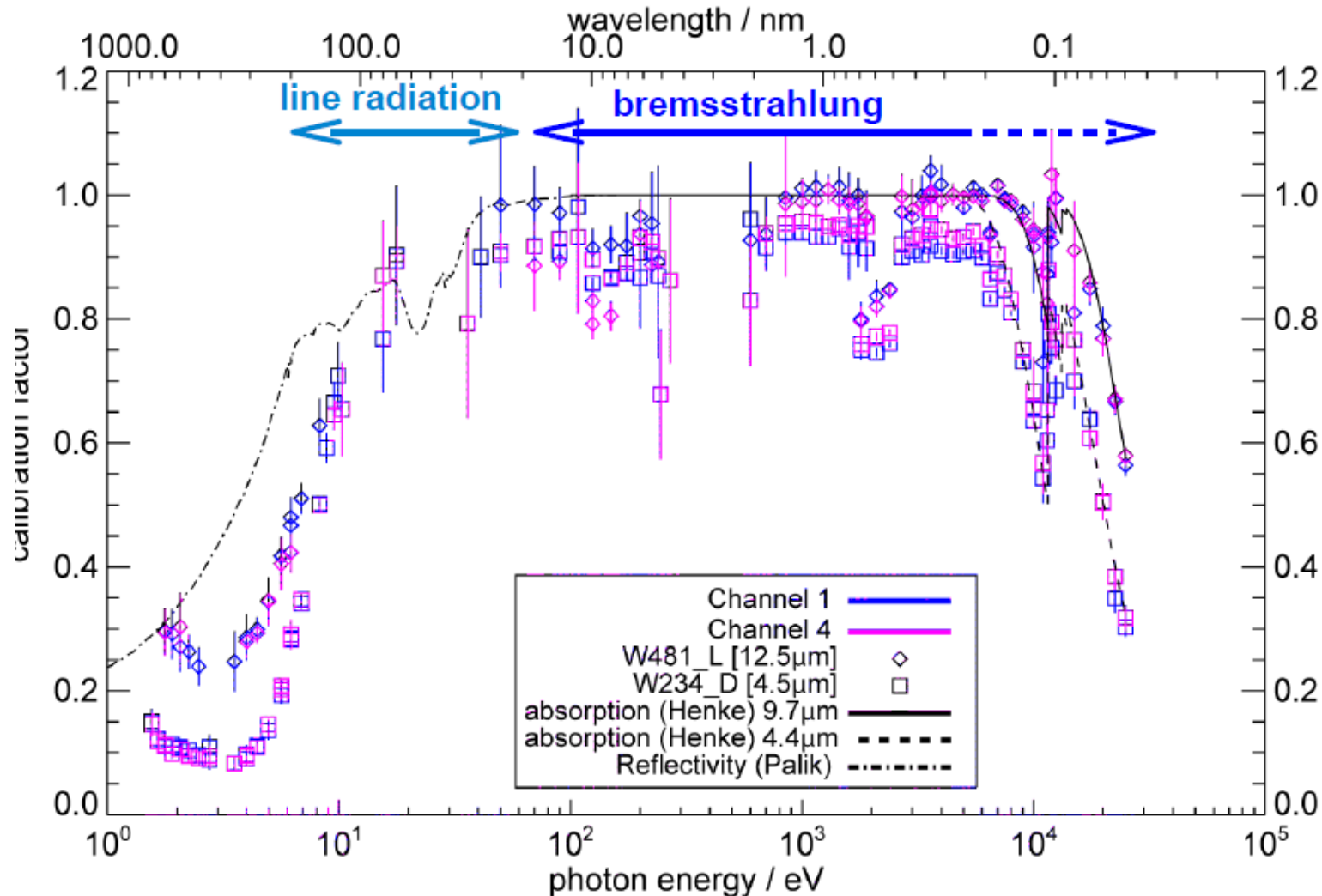
- Bolometers measure the plasma radiation, part of the energy balance:

$$P_{\alpha} + P_{ext} = P_{loss} + P_{rad}$$



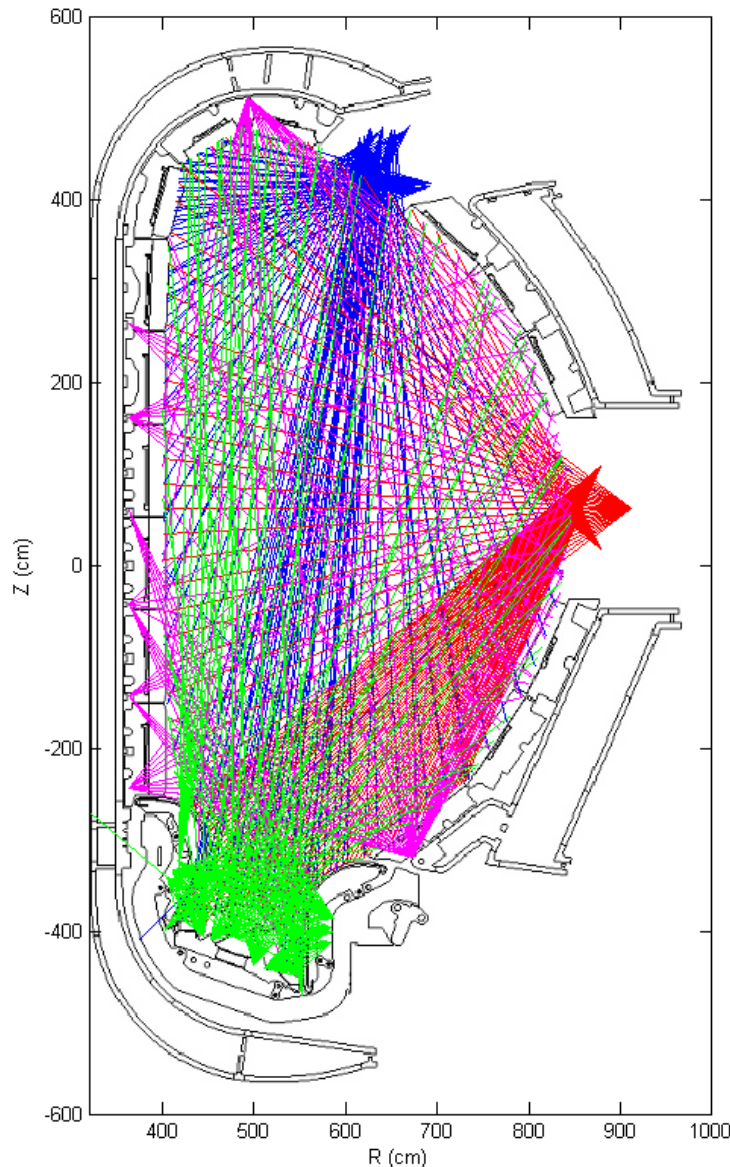
- Plasma radiation increases temperature of absorber
- Metal resistor detects temperature increase
- To compensate temperature changes from environment, additional reference absorber – shielded from plasma radiation – is used

Spectral sensitivity range of bolometers



The diagnostic is the most important contributor to the measurement of the total radiated power

[H. Meister , IPP Garching, Ringberg seminar 18.4.2013]



Emphasis is on divertor area (5 cm) monitoring of the detachment of the divertor plasma and the formation of X-Point-MARFES.

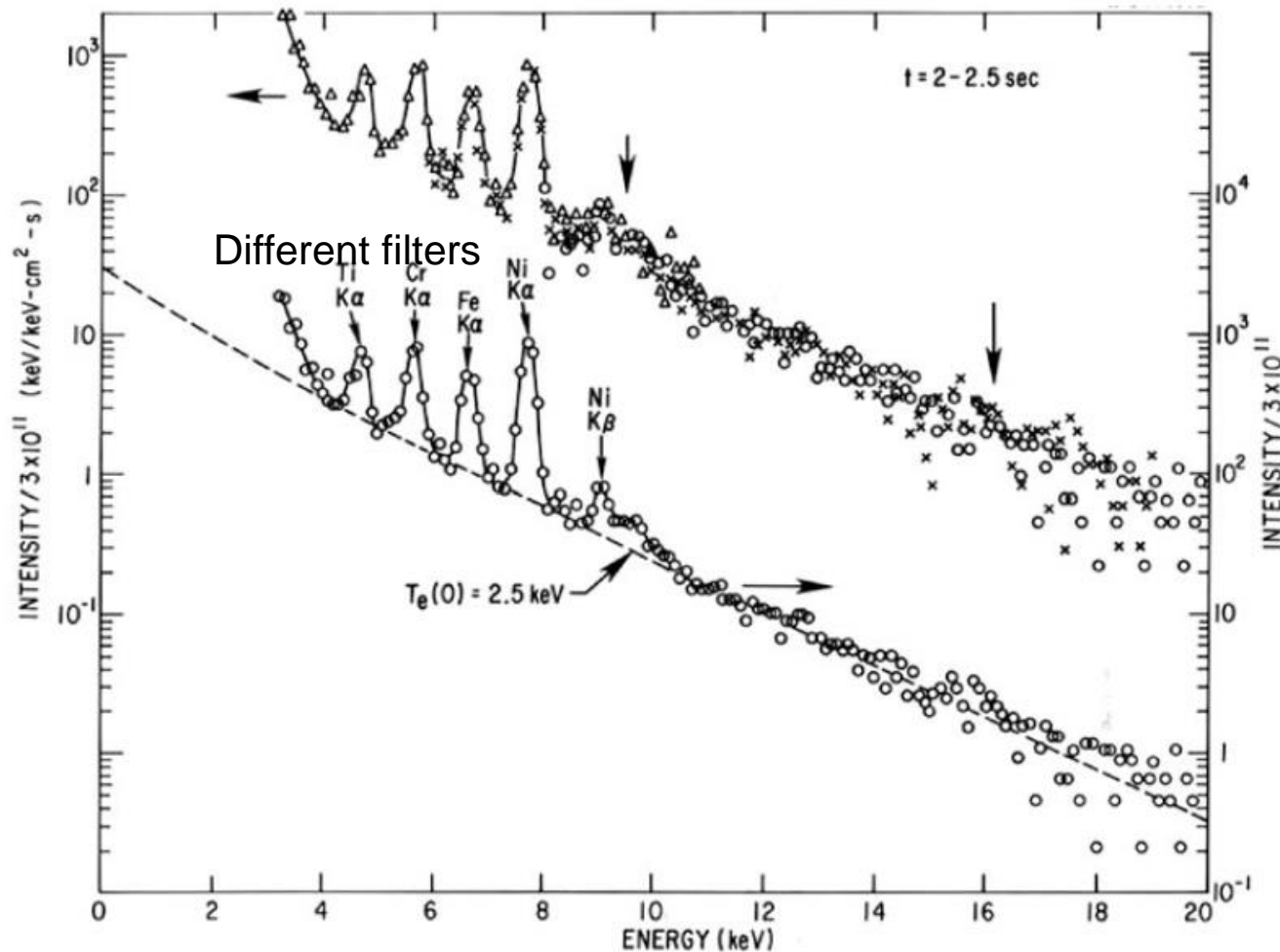
But also good resolution of main plasma area ($1/30^{\text{th}}$ of the minor plasma radius) for studying the edge radiation profile in various areas of the plasma, the upper target area, radiation phenomena related to transport barriers or impurity transport and accumulation in the centre and the temporal evolution of MARFES.

Total Radiation is a very robust measurement and does need only a small subset of the LOS. The profiles will need tomographic reconstructions. For this we are in sparse data domain.

For tomography the LOS need to be toroidally clustered together.

Some toroidal resolution is however also needed for disruption mitigation investigations.

Spectroscopy in the plasma core – Pulse high analysis SXR spectra in TFTR



K. Hill et al.,
Rev. Sci. Instr.
1985

From the measured
Bremsstrahlung
background, the
electron temperature
and electron density
can be determined:

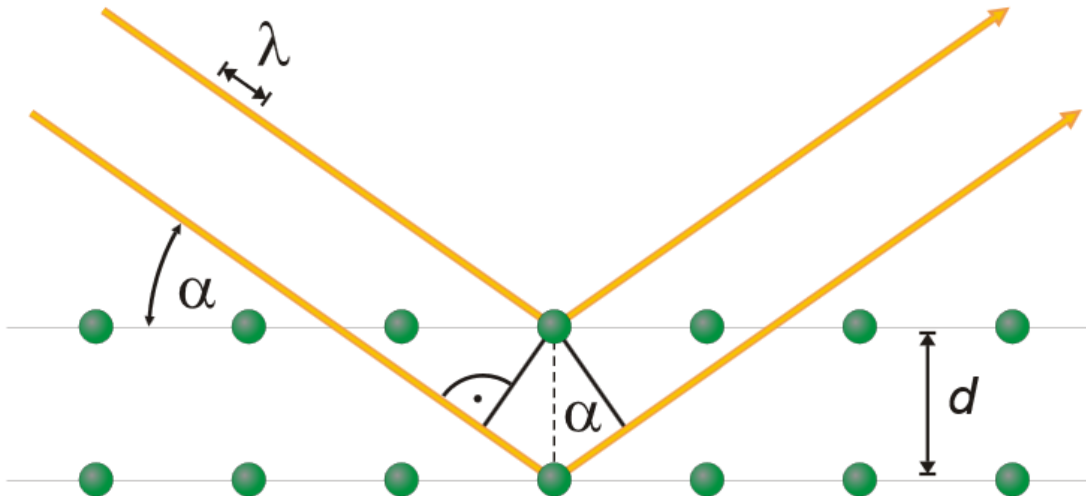
$$I_{\omega} d\omega \propto e^{\frac{\hbar\omega}{kT_e}} d\omega$$

and

$$I \sim n^2$$

(low spectral resolution via measurement of charge pulses generated from photon energies deposited in the semiconductor detector)

Using Bragg reflection for wavelength separation:



$$n \lambda = 2 d \sin \alpha$$

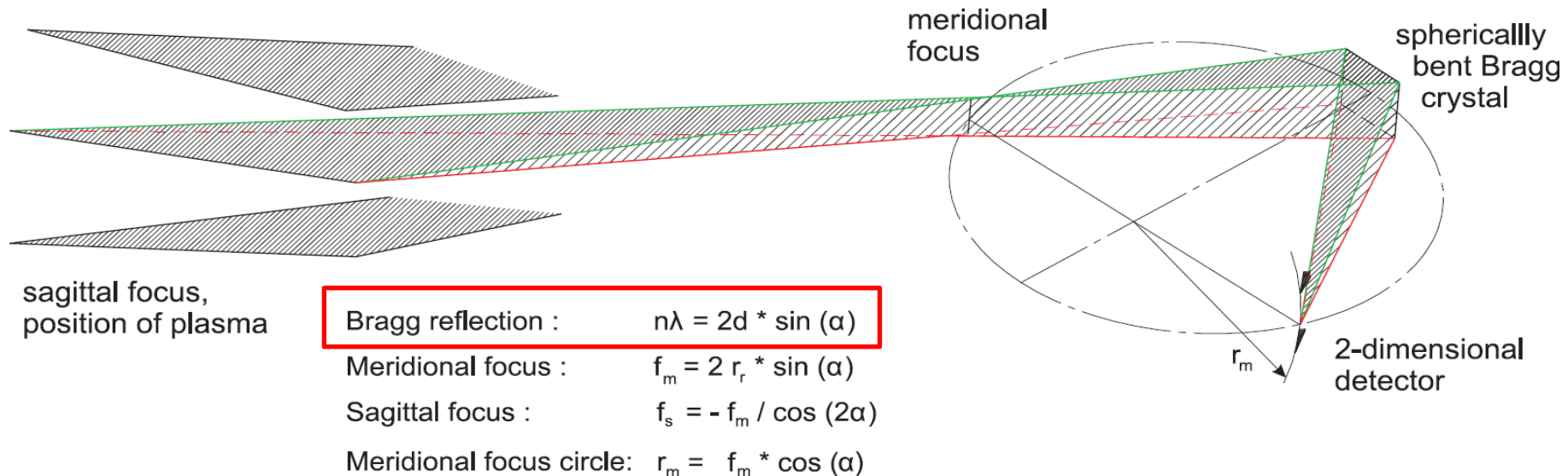
(image source: <https://lp.uni-goettingen.de/get/image/1539>)

Advantages of Bragg crystal spectroscopy:

- Good reflectivity in the x-ray wavelength range
- Very high spectral resolution possible due to small distance of planes d

(G. Bertschinger, O. Marchuk)

Bragg reflection in a perfect crystal can be used for wavelength separation:

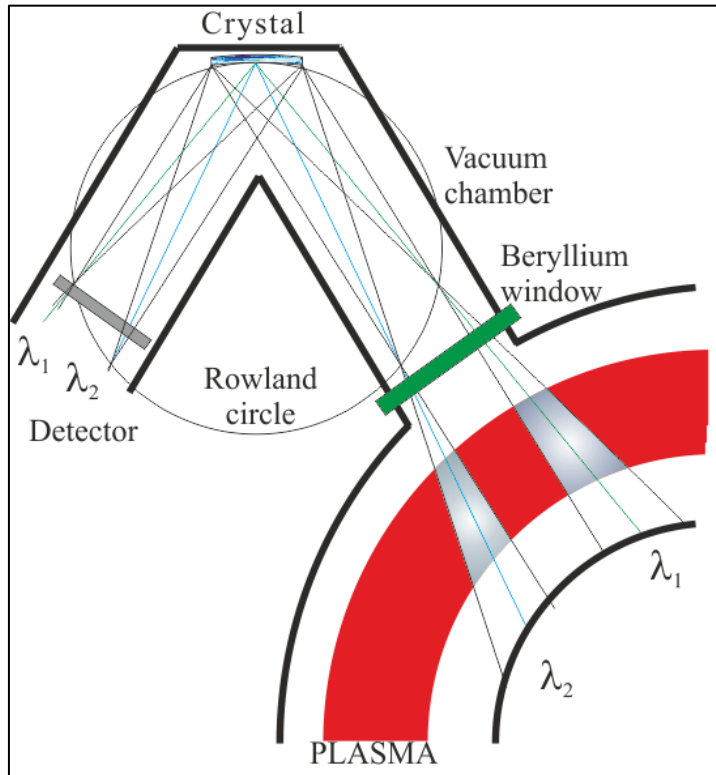


Modified Johann spectrometer:

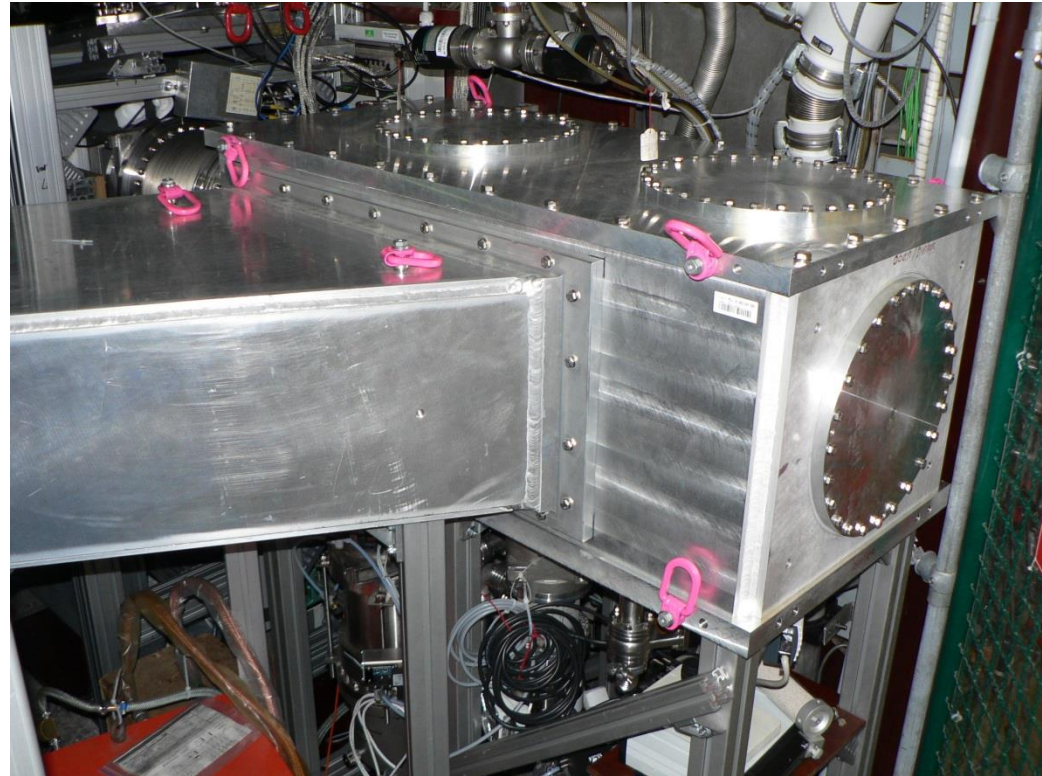
- Spherically bent crystal used to image the plasma light onto the 2-D detector (wavelength axis and radial coordinate)
- Spectral resolution governed by Bragg condition and by Rocking curve (crystal reflectivity as function of wavelength//angle)

(G. Bertschinger, O. Marchuk)

Principle:

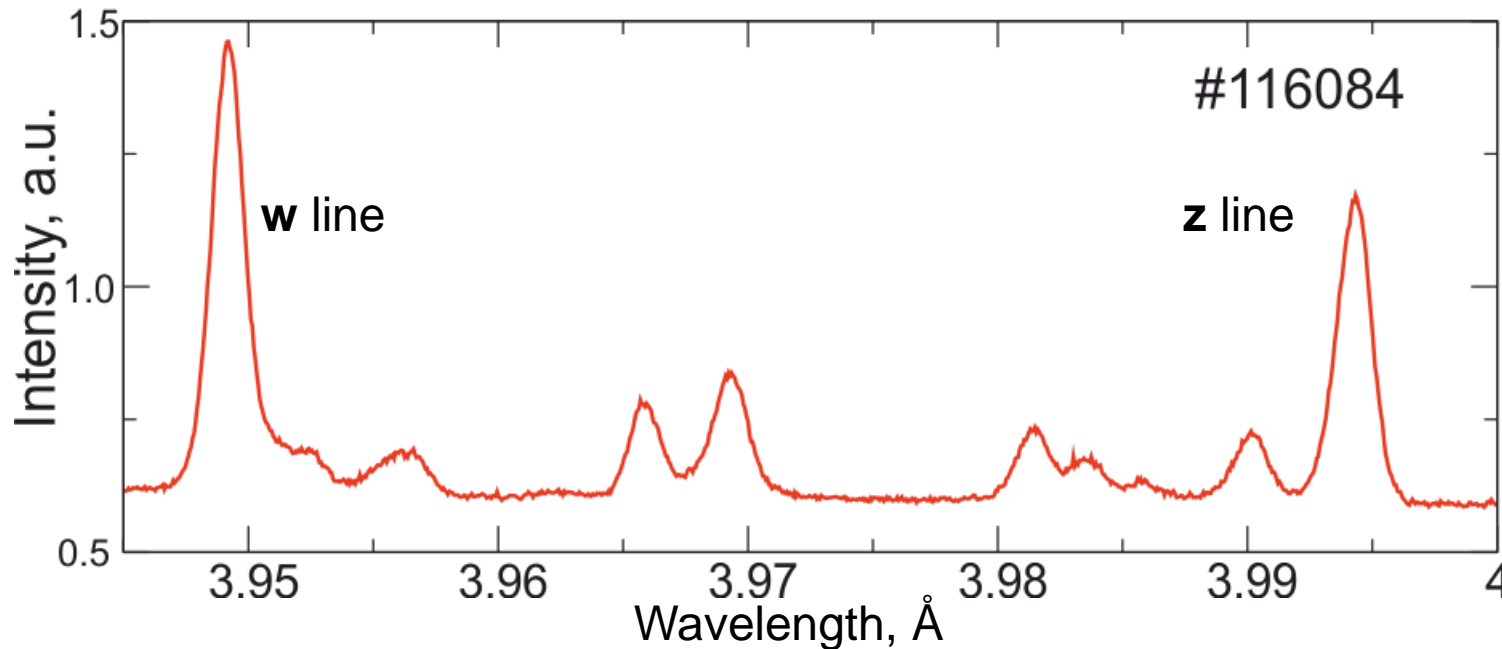


Bragg spectrometer on TEXTOR (2008):



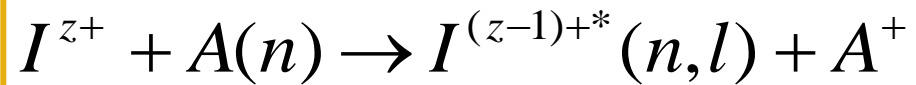
Example for x-ray spectra: He-like Argon (Ar^{16+})

(G. Bertschinger, O. Marchuk)



- The He-like x-ray spectrum consists of several components, which are excited via different processes
- The ion temperature can be derived from Doppler broadening
- The electron temperature can be obtained from line intensity ratios

Process:



FWHM

$$T_i = \frac{m_i}{k_B} \left(\frac{c \lambda_w}{\lambda_0 \sqrt{8 \ln 2}} \right)^2$$

Ion temperature

Line shift:

$$v_{rot} = -c \frac{\Delta \lambda_{rot}}{\lambda_0}$$

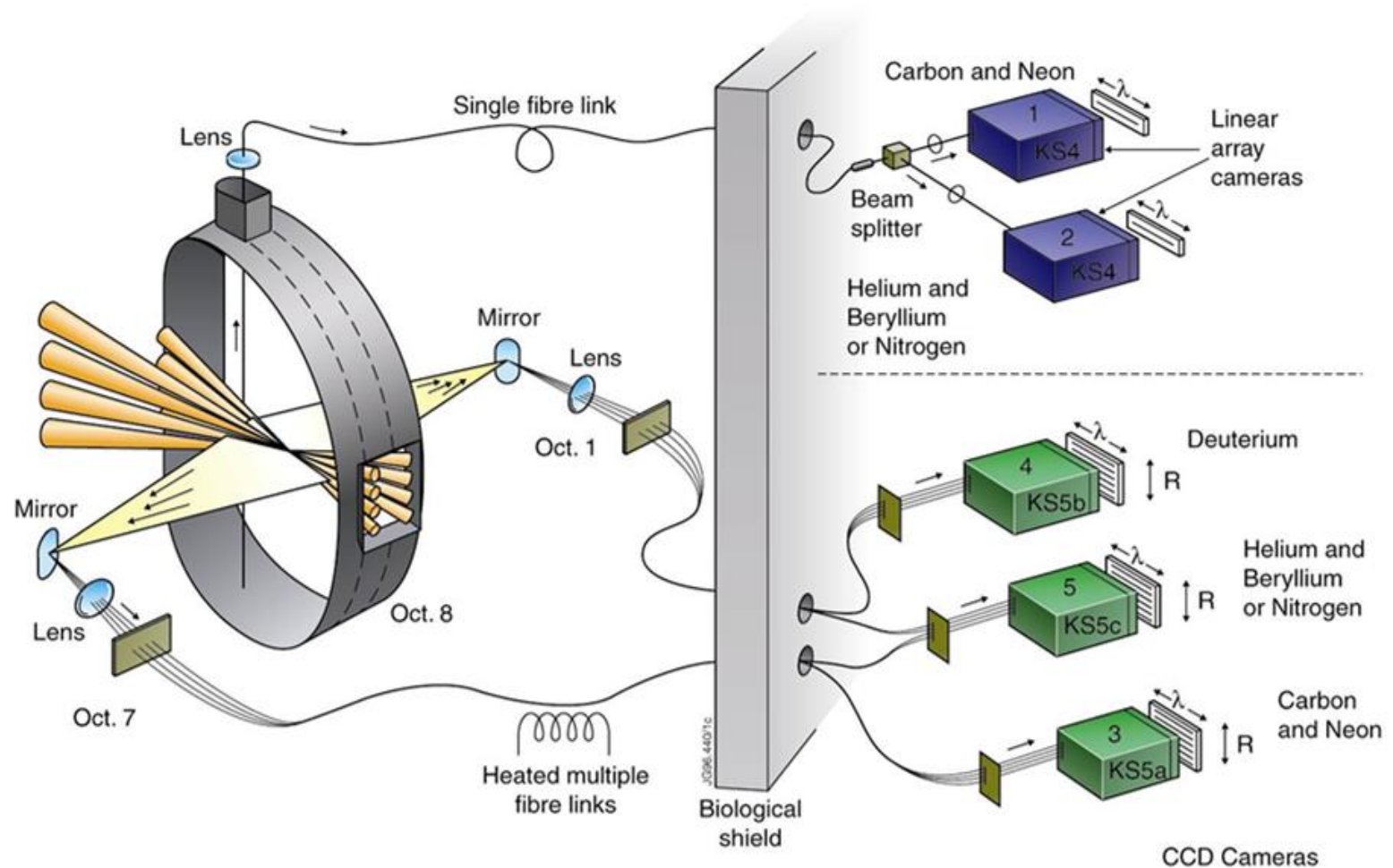
Rotation

integral

$$\phi = \frac{1}{4\pi} \int n_{I^{z+}} n_{beam} \langle \sigma_{em} v_{beam} \rangle d\ell$$

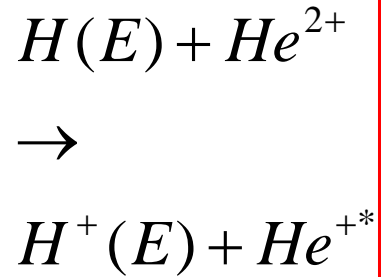
Impurity density

Core CXRS diagnostic at JET



Courtesy: Carine Giroud

ITER core CXRS diagnostics

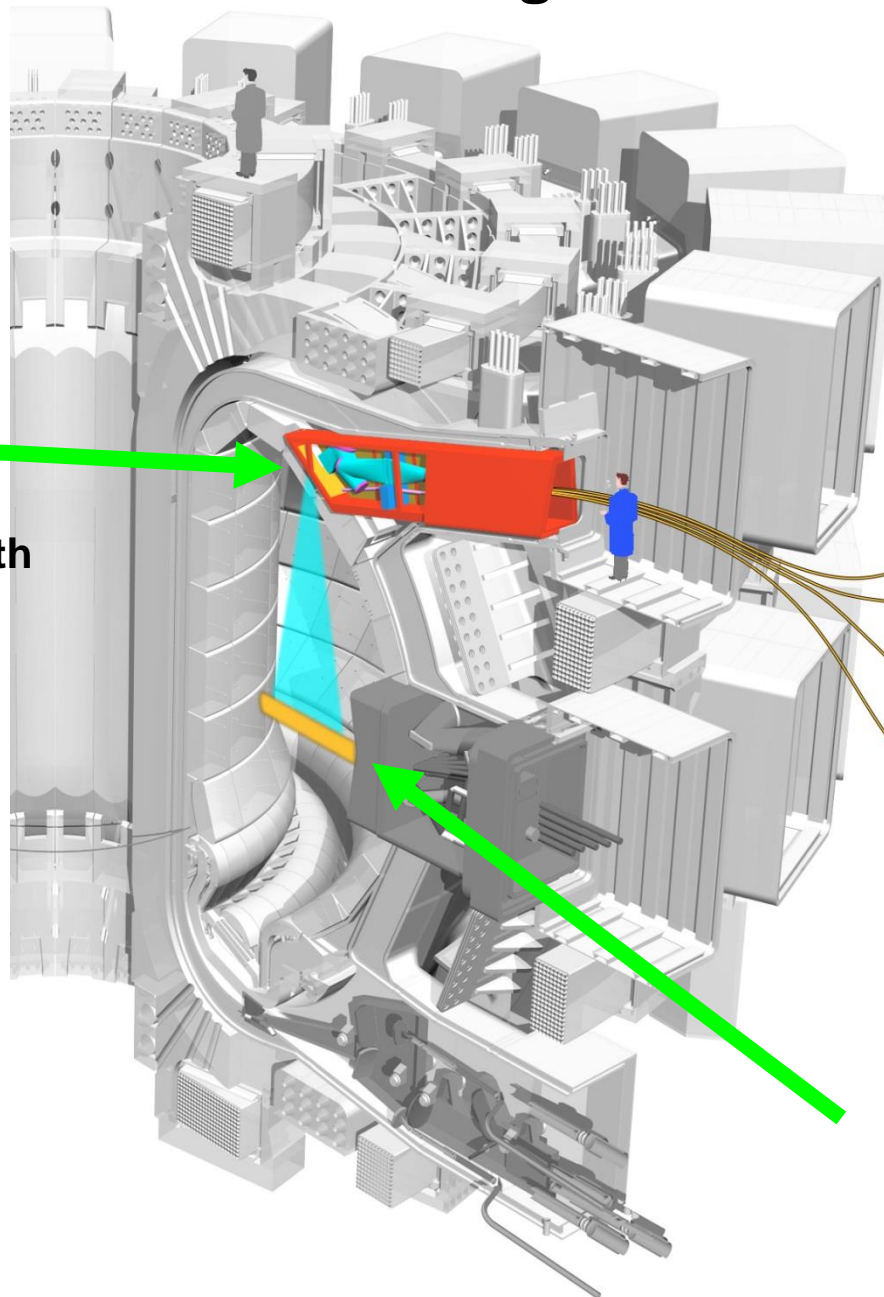


Measurement of
 n_{He} , T_i , v_{rot} , Z_{eff} ,
 n_{Be} , B , D/T

CXRS spectrometers

CXRS port plug
with mirror labyrinth

Hydrogen Injector (100 keV)



Multi-Device-CX-Spectra- Simulation (V5.20)

negative ion source

ITER Upper Port 3

Spectrometer Settings

quantum efficiency [%]

F-number

Optical Throughput

integration time [s]

slitwidth [mm]

slitheight [mm]

dispersion [Å/pixel]

binning

pixels

pixelsize [microns]

Beam Parameters

E [keV/amu] Ineut [Å]

div [mrad]

f(E) f(E/2) f(E/3)

blanket aperture(m) H W

tilt DNB [°] rotate DNB [°]

up/down acw/cw

Active Spectrum

CX-Line **Hell (4-3)** ☐ Fix Ti & Omega

Passive components

Edge-amplitude [a.u.] Ti-edge [eV]

PCX-component **Free parameters**

nd at boundary [10¹⁶ m⁻³] ☐ Show PCX model

Plasma Parameters

Ti(0) [keV] alpha-Ti

Te(0) [keV] alpha-Te

ne(0) [10²⁰ m⁻³] alpha-ne

vtor(0) [km/s] alpha-Om

vpol(0) [km/s] Sm_q Sm_p

rho (r/a)

Concentrations (%)

He+2 Be+4 C+6 Si+14 Ar+18

N+7 O+8 Ne+10 Ar+16

Ion Concentration Profile

Spectral Fit Results

vobs : -102.5 km/s; error = -65.2km/s

Ampl : 1.19e+013 ph/m²/sr/s/Å; error= 11.46%

Base : 6.59e+015 ph/m²/sr/s/Å; error= 0.01%

Ti : 20.6405 keV; error=5.37%

<SNR at half ampl> : 2.3284 ☐ Show Optimisation

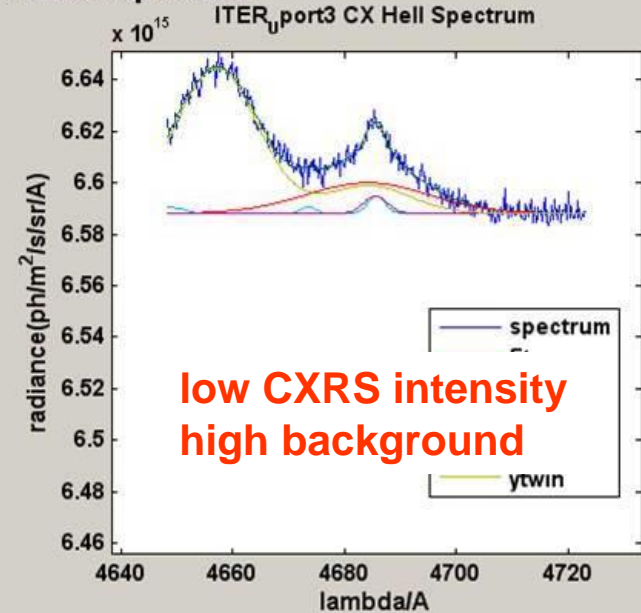
NB ModulationNo

Output File

start calculation

exit

Calculated spectrum



☐ Show Raw Data

☐ ShowCXeffect

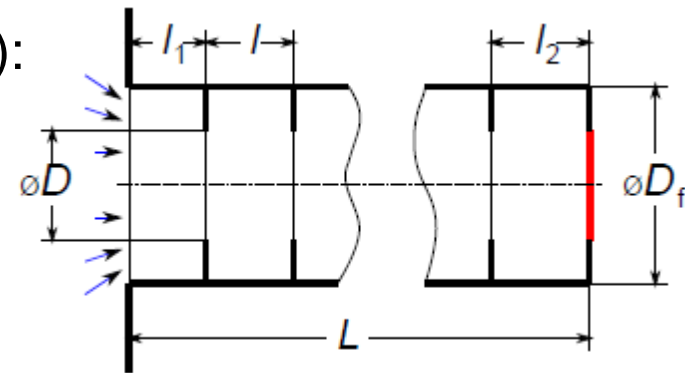
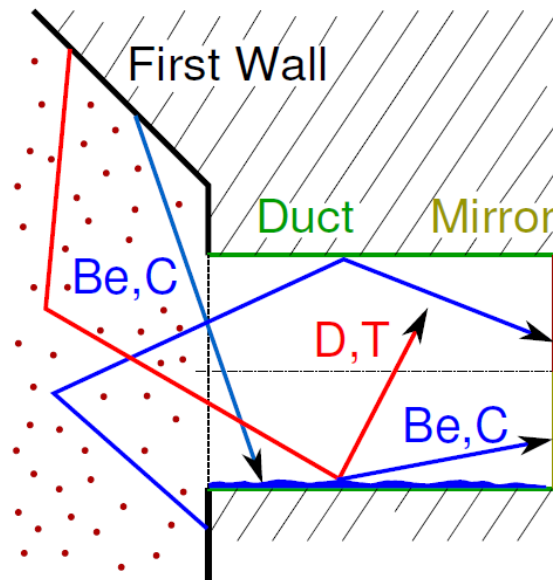
Required accuracy for n_{He}: 10%

- atomic data
- absolute calibration
- statistical errors

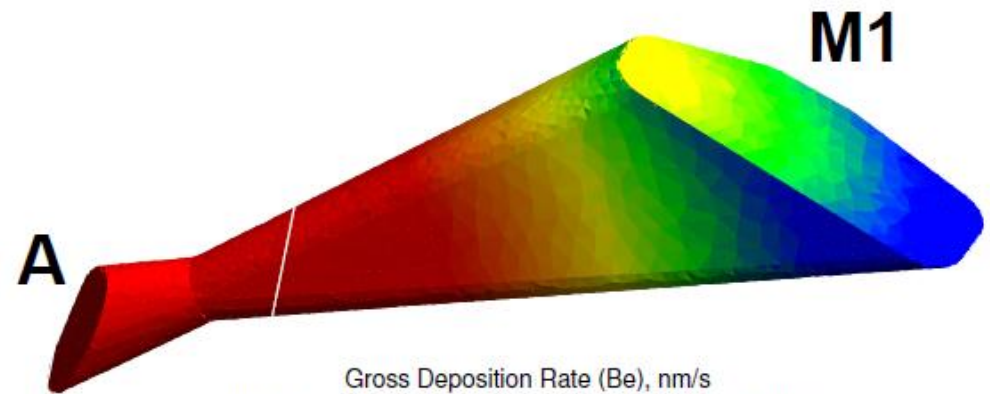
multiplet ratio : 5:3:1

Neutral particle and ion fluxes for hydrogen isotopes and impurities are modelled using the B2-EIRENE code package.

Principle geometry (with baffles):

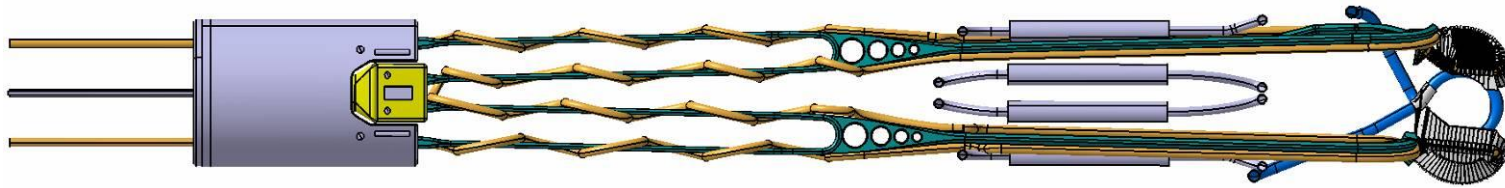


(first mirror)

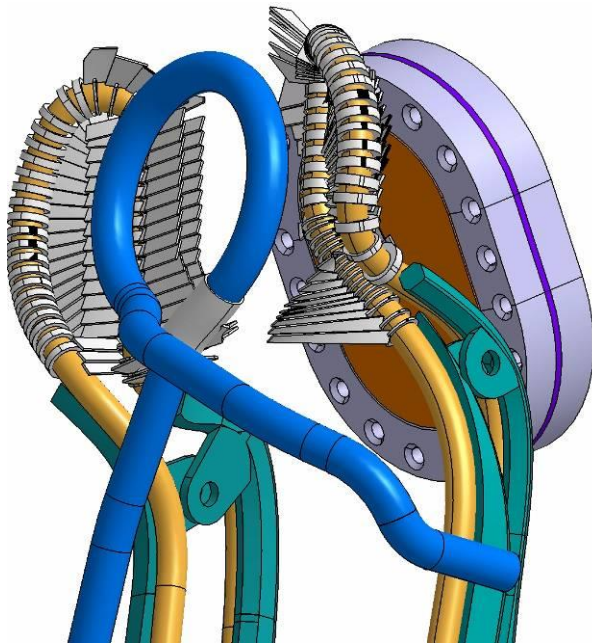


(aperture)

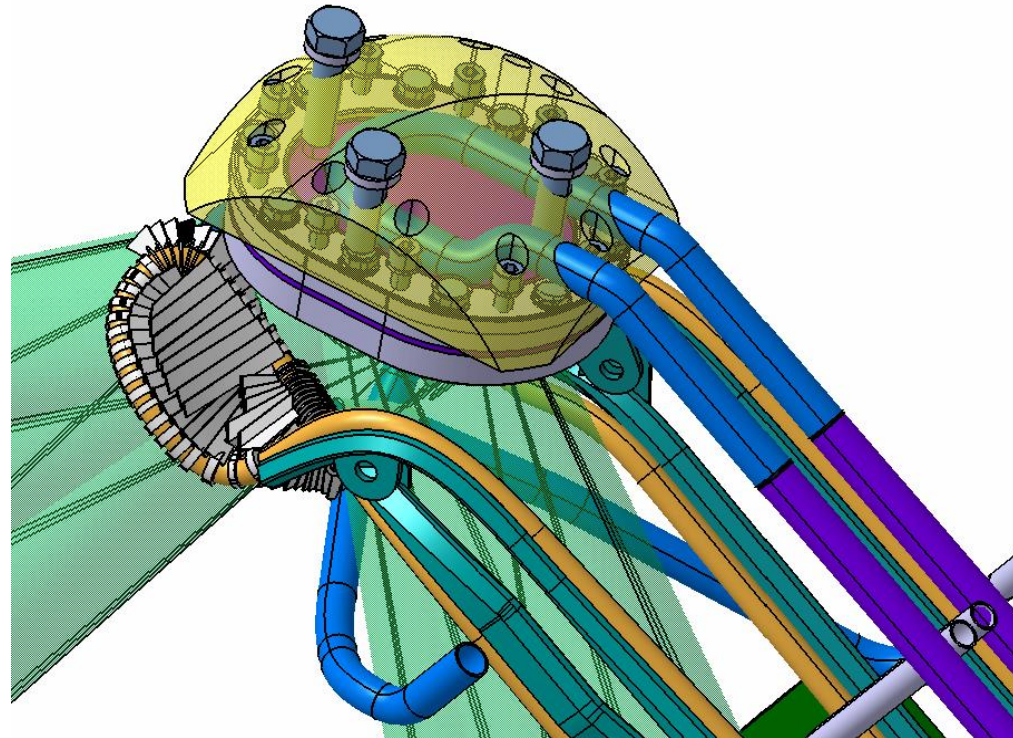
Gross Deposition Rate (Be), nm/s
 $2e-05$ $3.2e-05$ $5e-05$ $8e-05$ 0.00013 0.0002



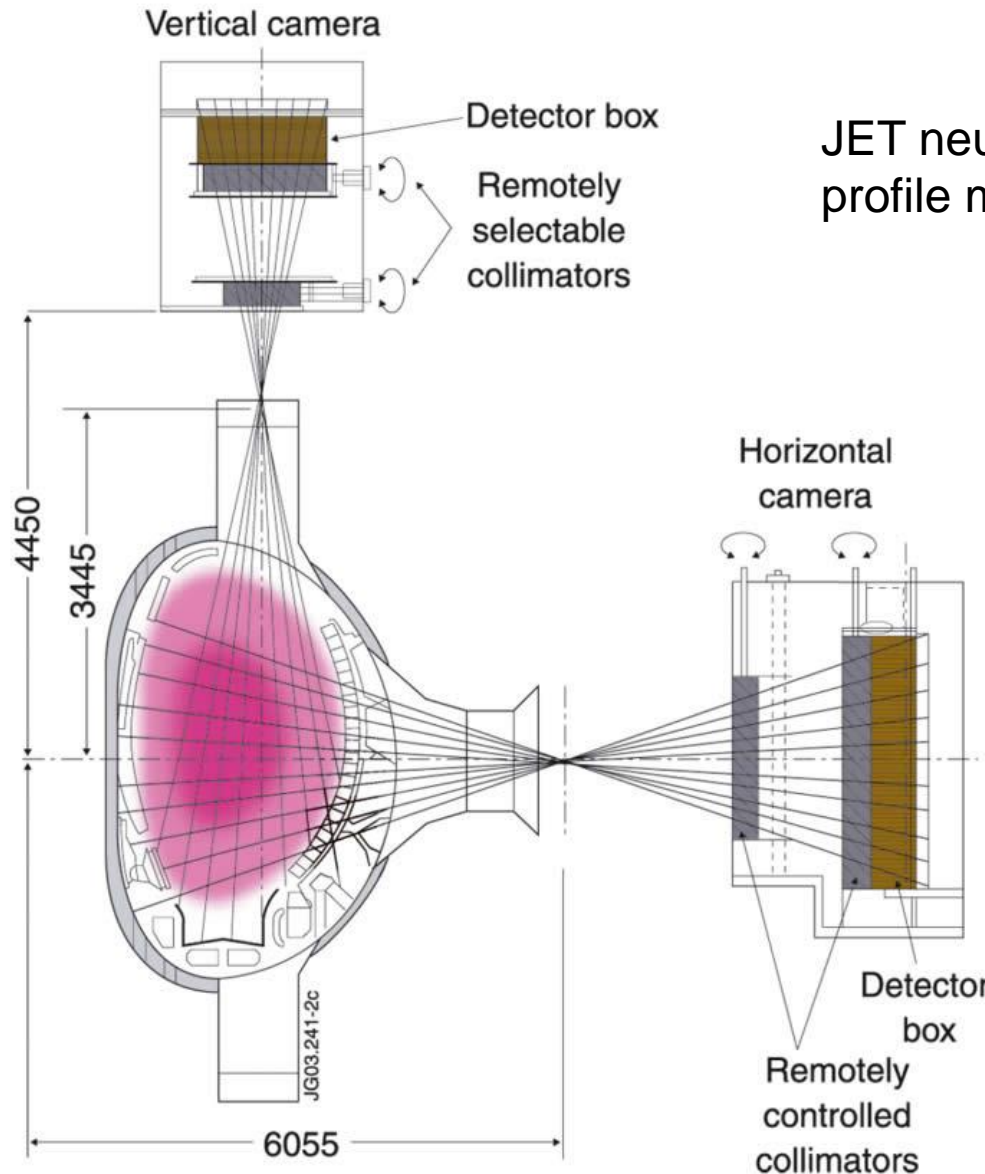
shutter with
flaps and
actuator



mirror 1 attachment with thermal
conditioning loops, shutter flaps
and alignment screws



Passive diagnostics: example of neutron detection w/o probing beams or lasers



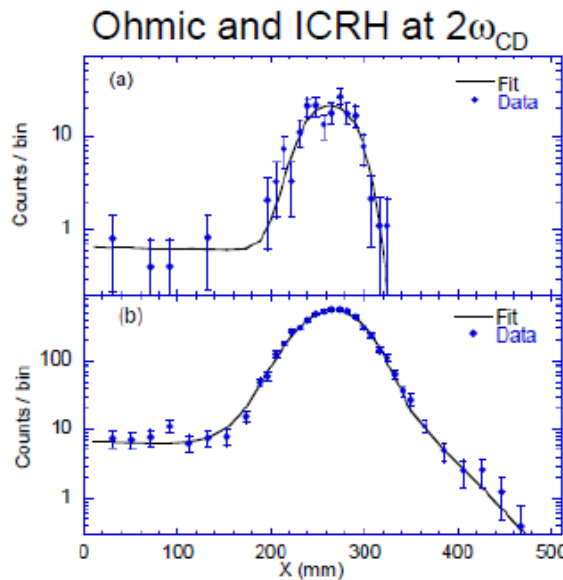
JET neutron / gamma
profile monitor

Allows measurement of:

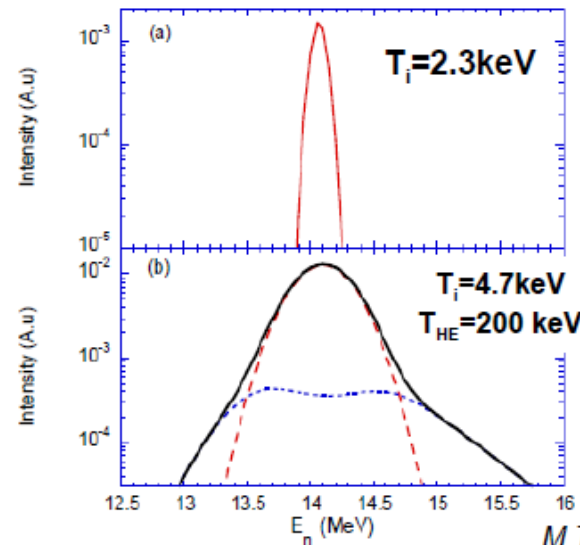
- fusion power density
- n, Ti profiles
- Ti from neutron spectra

Neutron spectroscopy of DT plasmas

(M. Tardocchi et al.)



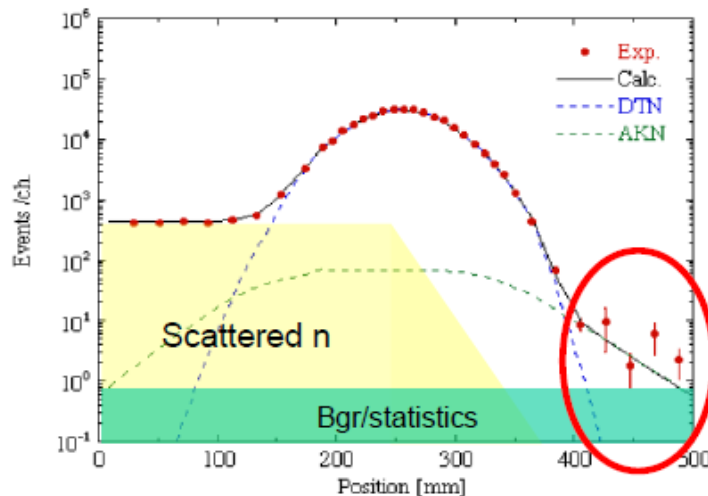
Spectral components inferred from fit



**Measure tail
temperature of fast D**

M. Tardocchi, PhD thesis, Uppsala (2000)

Alpha heating in DT; MPR 1997



Alpha knock-on signatures in the neutron spectrum

Weak component

Measure fusion α .

J. Kaellne et al, PRL 85(2000)1246

- **A) Technical goals of plasma diagnostics:**
 - *Protection of the fusion reactor and its components*
 - e.g. distance between plasma and first wall, wall temperature, fusion power
 - *Control and optimisation of the plasma properties*
 - e.g. plasma shape, plasma position, plasma current, plasma density, impurity concentrations, radial distributions of plasma quantities
 - *Plasma physics studies (obtain data to be used for as basis for concept improvements)*
 - All plasma quantities
- **B) Diagnostic methods / measurement principles:**
 - *Magnetic measurements*
 - *Neutron and gamma diagnostics*
 - *Optical / IR diagnostics*
 - *Bolometric diagnostics*
 - *Spectroscopic techniques*
 - *Microwave diagnostics*
 - *Plasma-facing components and operational diagnostics*

Outline of a control concept for a fusion reactor

No.	Control function	Relevance / operational limits	DEMO1	DEMO2
1.	Plasma current, position and shape control			
1.1.	Plasma current	q95 limit	Global	Profile
1.2.	Gaps (LCFS position at a number of poloidal locations) and divertor strike points	Wall loads	X	X
1.3.	Vertical stability	Wall loads / disruption avoidance	X	X
2.	Kinetic control			
2.1.	Core density	Density limit	Global	Profile
2.2.	Fusion power	Wall load	X	X
3.	Exhaust control			
3.1.	Core radiation	Radiation limit / H mode threshold	X	X
3.2.	$P_{\text{SOL}} > P_{\text{LH}}$; edge radiation	H mode threshold / Divertor loads	X	X
3.3.	First wall loads	1st wall loads	X	X
3.4.	Divertor radiation and detachment control	Radiation limit / Divertor loads	X	X
3.5.	Divertor target peak loads + temperatures	Divertor loads	X	X
4.	MHD control			
4.1.	Sawtooth instability	Confinement / disruption avoidance	X	X
4.2.	Neoclassical tearing modes	Confinement / disruption avoidance	X	X
4.3.	Locked modes	Confinement / disruption avoidance	X	X
4.4.	Edge localised modes	Confinement / disruption avoidance	X	X
4.5.	Beta limit	Confinement / disruption avoidance	n.a.	X
5.	Event handling			
5.1.	Impurity release	Radiation limit / wall loads	X	X
5.2.	Control failure	Disruption avoidance/mitigation	X	X
5.3.	Disruption mitigation	Limitation of machine damage	X	X
5.4.	Runaway electron occurrence	Limitation of machine damage	X	X

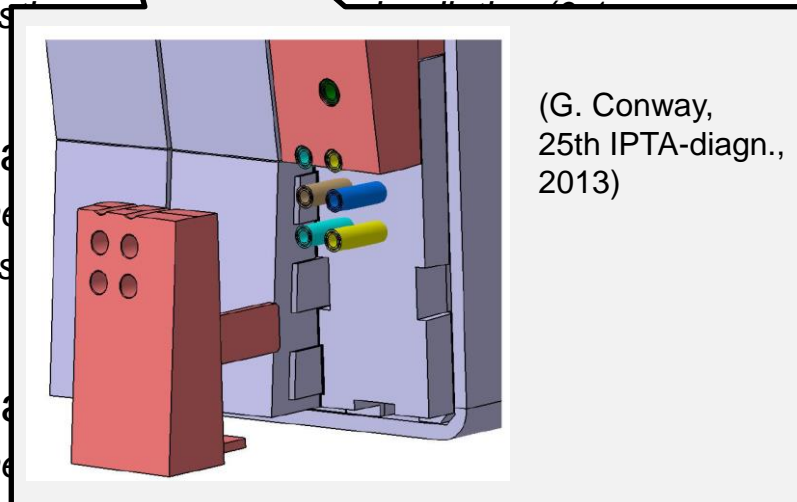
Diagnostics which are most likely feasible:

- Microwave diagnostics (reflectometry, ECE)
 - *Measurements:* n_e (gradient region), T_e , plasma position and shape, instabilities
 - *Characteristics:* mm waves, robust front-end (horn antenna + metallic waveguide)
 - *Problems:* location and shape of antennae might need to be adapted to optimisation of TBR and to maximisation of lifetime, reducing gain and signal quality
- Polarimetry/interferometry
 - *Measurements:* n_e (plasma core)
 - *Characteristics:* far infrared radiation (0.1 mm waves), retro-reflectors deep in blanket (?)
 - *Problems:* large beam diameter, beam duct requiring blanket modification
- Neutron + gamma diagnostics
 - *Measurements:* fusion power density, contribute to $n + T_i$ profiles, T_i from neutron spectra
 - *Characteristics:* need only tube-like access, detectors can be placed behind the shield
 - *Problems:* difficult analysis of data (variety of processes, neutron scattering)
- Plasma radiation / spectroscopy
 - *Measurements:* impurity composition (Z_{eff}), P_{rad} , divertor thermography, T_i (?), v_{rot} (?)
 - *Characteristics:* tube-like access, first mirror behind blanket
 - *Problems:* Low etendue, low coverage, low performance

Feasible
Low performance
Critical

Diagnostics which are most likely feasible:

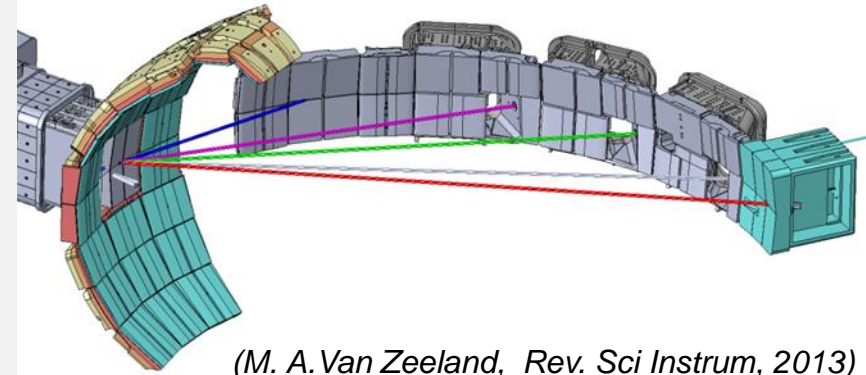
- Microwave diagnostics (reflectometry, ECE)
 - Measurements: n_e (gradient region), T_e , plasma position and shape, instabilities
 - Characteristics: mm waves, robust front-end (horn antenna + metallic waveguide)
 - Problems: location and shape of antennae might need to be adapted to optimisation of TBR and to maximisation of lifetime, reducing gain and signal quality
- Polarimetry/interferometry
 - Measurements: n_e (plasma core)
 - Characteristics: mm waves, retro-reflectors deep in blanket (?) requiring blanket modification
 - Problems:
- Neutron + gamma
 - Measurements: T_i profiles, T_i from neutron spectra
 - Characteristics: can be placed behind the shield
 - Problems: processes, neutron scattering
- Plasma radiation
 - Measurements: for thermography, T_i (?), v_{rot} (?)
 - Characteristics: tube-like access, first mirror behind blanket
 - Problems: Low etendue, low coverage, low performance



Feasible
Low performance
Critical

Diagnostics which are most likely

- Microwave diagnostics (reflectometry)
 - Measurements: n_e (gradient measurement)
 - Characteristics: mm waves
 - Problems: location of antenna
- Polarimetry/interferometry
 - Measurements: n_e (plasma core)
 - Characteristics: far infrared radiation (0.1 mm waves), retro-reflectors deep in blanket (?)
 - Problems: large beam diameter, beam duct requiring blanket modification
- Neutron + gamma diagnostics
 - Measurements: fusion power density, contribute to $n + T_i$ profiles, T_i from neutron spectra
 - Characteristics: need only tube-like access, detectors can be placed behind the shield
 - Problems: difficult analysis of data (variety of processes, neutron scattering)
- Plasma radiation / spectroscopy
 - Measurements: impurity composition (Z_{eff}), P_{rad} , divertor thermography, T_i (?), v_{rot} (?)
 - Characteristics: tube-like access, first mirror behind blanket
 - Problems: Low etendue, low coverage, low performance



(M. A. Van Zeeland, Rev. Sci Instrum, 2013)

Feasible
Low performance
Critical

Diagnostics whi

- Microwave dia

- Measurement
- Characteristic
- Problems:

- Polarimetry

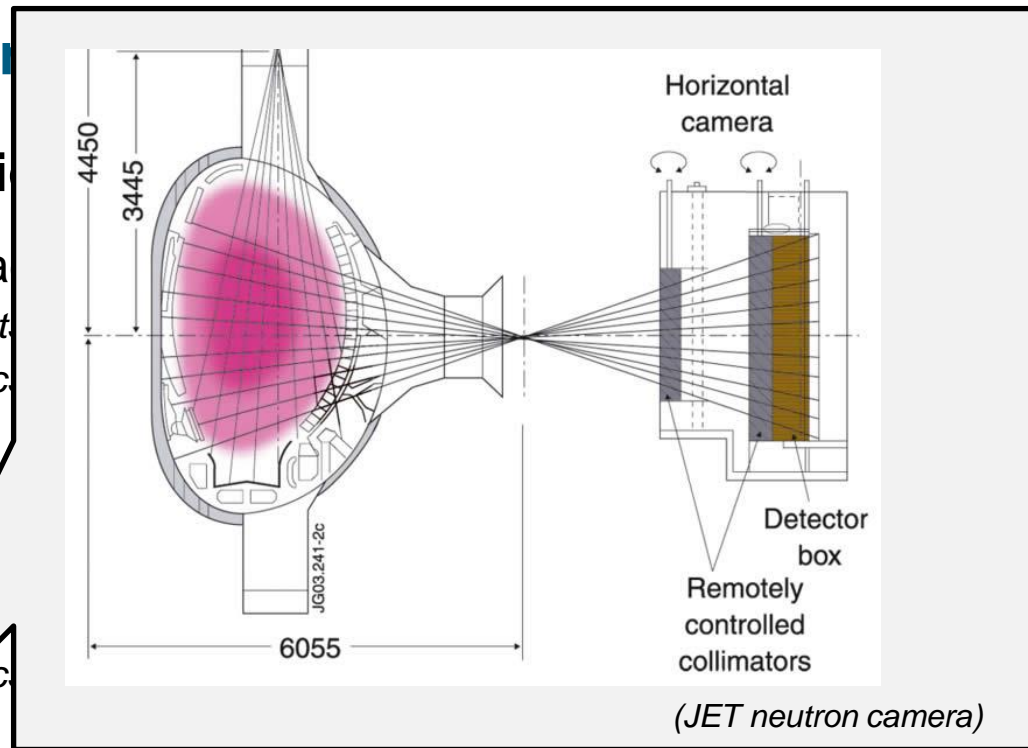
- Measure
- Characteristic
- Problems:

- Neutron + gamma diagnostics

- Measurements: *fusion power density, contribute to $n + T_i$ profiles, T_i from neutron spectra*
- Characteristics: *need only tube-like access, detectors can be placed behind the shield*
- Problems: *difficult analysis of data (variety of processes, neutron scattering)*

- Plasma radiation / spectroscopy

- Measurements: *impurity composition (Z_{eff}), P_{rad} , divertor thermography, T_i (?), v_{rot} (?)*
- Characteristics: *tube-like access, first mirror behind blanket*
- Problems: *Low etendue, low coverage, low performance*



*stabilities
waveguide)
adapted to optimisation
and signal quality*

*deep in blanket (?)
modification*

Feasible
Low performance
Critical

Diagnostics which are most likely feasible:

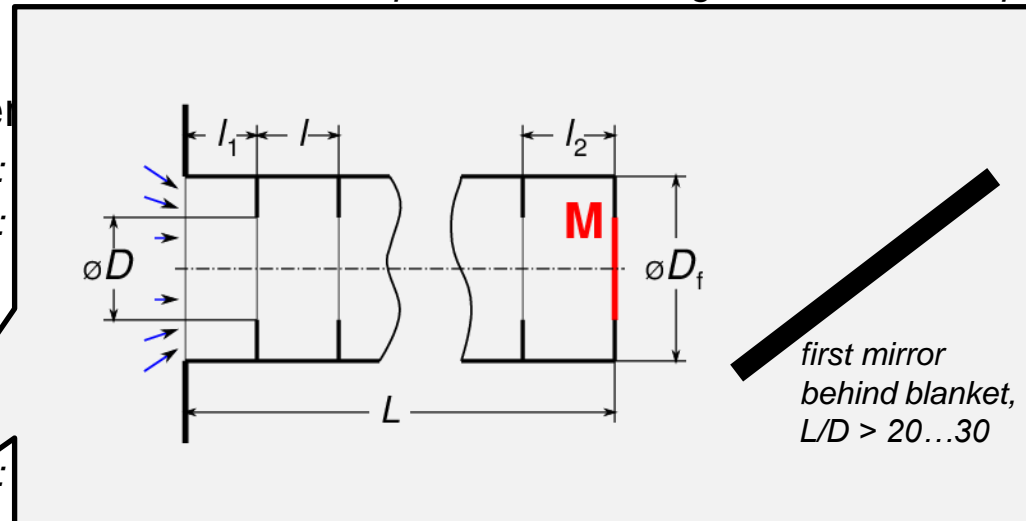
- Microwave diagnostics (reflectometry, ECE)
 - Measurements: n_e (gradient region), T_e , plasma position and shape, instabilities
 - Characteristics: mm waves, robust front-end (horn antenna + metallic waveguide)
 - Problems: location and shape of antennae might need to be adapted to optimisation and signal quality

- Polarimetry/interferometry

- Measurements:
 - Characteristics:
 - Problems:

- Neutron + gamma

- Measurements:
 - Characteristics:
 - Problems:



step in blanket (?)
fication

on neutron spectra
hind the shield

difficult analysis of data (variety of processes, neutron scattering)

- Plasma radiation / spectroscopy

- Measurements: impurity composition (Z_{eff}), P_{rad} , divertor thermography, T_i (?), v_{rot} (?)
 - Characteristics: tube-like access, first mirror behind blanket
 - Problems: Low etendue, low coverage, low performance

Feasible
Low performance
Critical

Diagnostics which are most likely feasible:

- Magnetic diagnostics

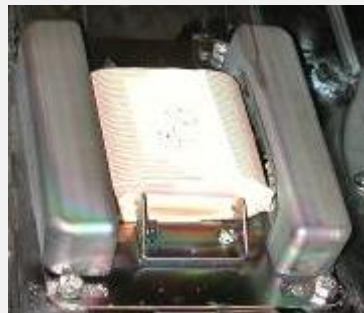
- *Measurements:* U_{Loop} , I_p , E_{Dia} , (plasma position and shape?)
- *Characteristics:* Magnetic sensors behind blanket/shield, Hall probes behind shield
- *Problems:* Low time resolution, long integration time

- FW and divertor

- *Measurements:* Absolute measurement of thermal power
- *Characteristics:* Sensors outside the tokamak
- *Problems:*

- Current density

- *Measurements:*
- *Characteristics:*
- *Problems:*



(typical pick-up coil)



(metallic Hall sensor prototype, I. Duran et al.)

- Measurements

- *Measurements:* slow and indirect
- *Characteristics:*
- *Problems:*

target plates

(A. Kallenbach et al., PPCF 2010)

, measurement of current + voltage
divertor load requirements (?)

exhaust

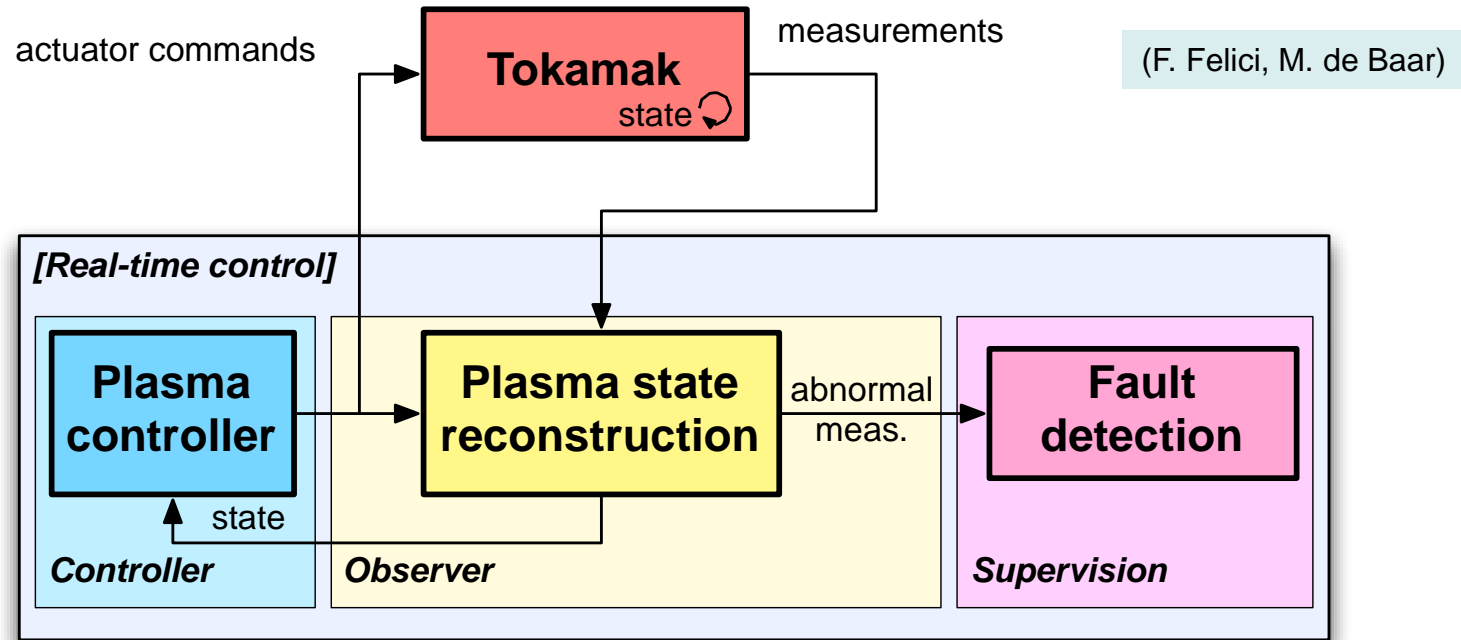
exhaust gas composition

Feasible
Low performance
Critical

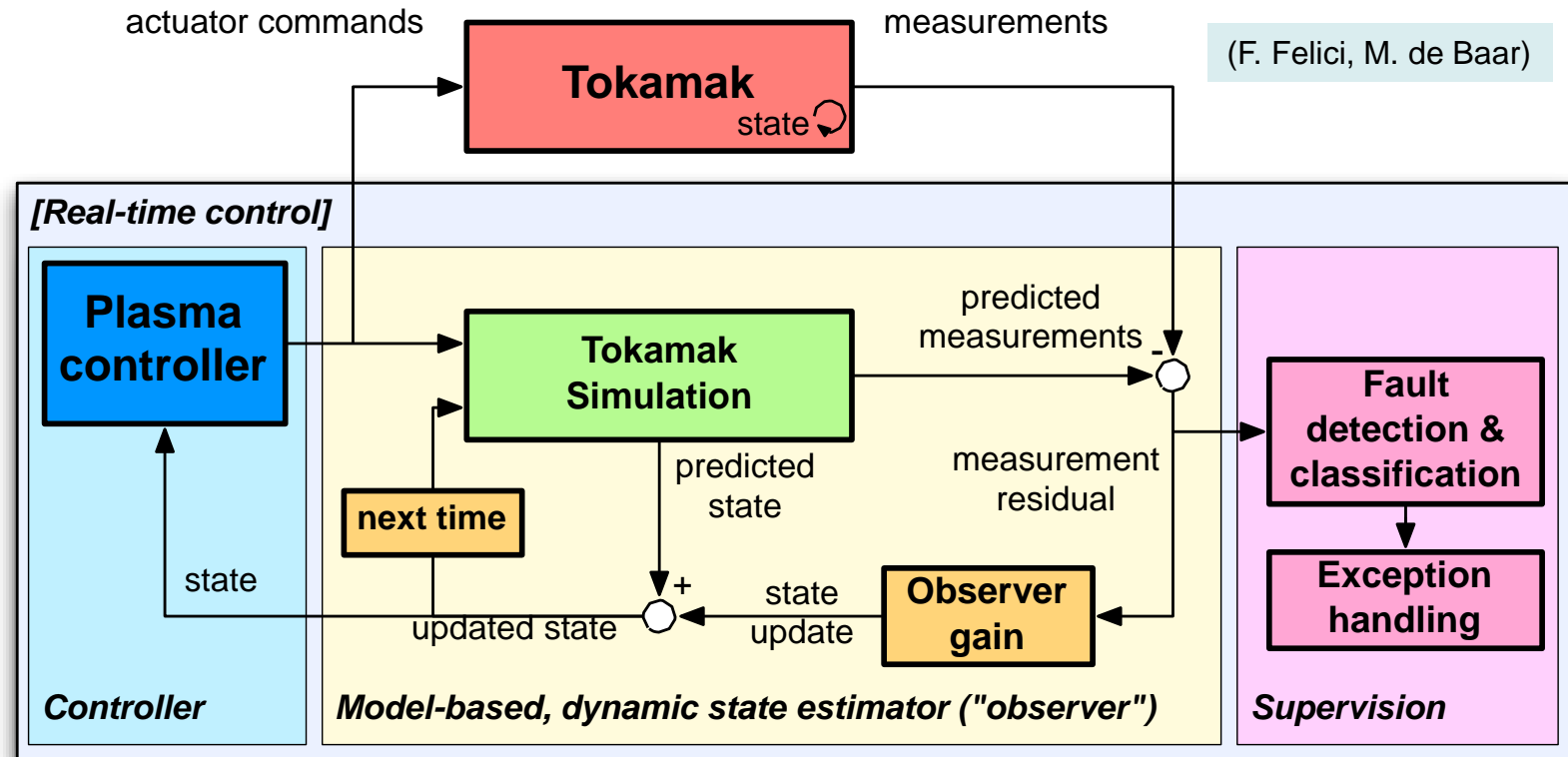
Diagnostics which are most likely feasible:

- Magnetic diagnostics
 - *Measurements:* U_{Loop} , I_p , E_{Dia} (*plasma position and shape?*)
 - *Characteristics:* Magnetic sensors behind blanket/shield, Hall probes behind shield
 - *Problems:* Low time resolution, long integration time
- FW and divertor coolant temperature, flow and pressure
 - *Measurements:* absolute measurement of thermal power
 - *Characteristics:* sensors outside the tokamak
 - *Problems:* slow and low spatial resolution
- Current density / voltage measurement at divertor target plates
 - *Measurements:* Perspective for detachment control (A. Kallenbach et al., PPCF 2010)
 - *Characteristics:* isolated mounting of divertor modules, measurement of current + voltage
 - *Problems:* *divertor scenario // compatibility with divertor load requirements (?)*
- Measurement of gas/beam/pellet fuelling and gas exhaust
 - *Measurements:* Injected particles, neutral pressure, exhaust gas composition
 - *Characteristics:* sensors in remote positions
 - *Problems:* slow and indirect

Feasible
Low performance
Critical



- Plasma controller: perform control actions based on full plasma state knowledge
- Plasma state reconstruction: derive plasma state by merging measurements from several diagnostics
- Fault detection: classify unexpected measurements (e.g. off-normal events, faulty signals)
- Diagnostic redundancy in number of channels and number of methods facilitates handling of faults (the better the model, the less measurements are needed)



- Run tokamak simulation in parallel with plasma evolution
- Correct simulated state estimate based on difference between predicted and true measurements
- Detection & classification of excessive discrepancies
- The plasma controller may initiate fast rampdown or disruption mitigation if a discrepancy cannot be resolved otherwise